Editors' Suggestion

Chiral coupling of magnons in waveguides

Tao Yu,[1] Xiang Zhang,[1] Sanchar Sharma,[1] Yaroslav M. Blanter,[1] and Gerrit E. W. Bauer[2,1]
[1]*Kavli Institute of Nanoscience, Delft University of Technology, 2628 CJ Delft, Netherlands*
[2]*Institute for Materials Research & WPI-AIMR & CSRN, Tohoku University, Sendai 980-8577, Japan*

(Received 7 September 2019; revised manuscript received 14 February 2020; accepted 18 February 2020; published 11 March 2020)

We theoretically investigate the collective excitations of multiple (sub)millimeter-sized ferromagnets mediated by waveguide photons. By the position of the magnets in the waveguide, the magnon-photon coupling can be tuned to be chiral, i.e., magnons only couple with photons propagating in one direction, leading to an asymmetric transfer of angular momentum and energy between the magnets. A large enhancement of the magnon number population can be achieved at an edge of a long chain of magnets. The chain also supports standing waves with low radiation efficiency that are inert to the chirality.

DOI: 10.1103/PhysRevB.101.094414

I. INTRODUCTION

Magnetic insulators are promising materials for low-dissipation information technology with magnons, the elementary excitation of magnetic order, rather than electrons [1–4]. The long lifetime of magnons in high-quality magnetic insulators such as yttrium iron garnet (YIG) [5] are suitable for data storage, logic, and medium-distance interconnects but cannot compete with photons in terms of speed and coherence lengths. Coupled magnon-photon systems are therefore promising for quantum communication over large distances [6]. The interface to conventional electronics are metal contacts that allow magnons to interact with conduction electrons by interfacial exchange interaction, giving rise to spin pumping and spin transfer torques [7,8]. Magnons in separate nanomagnets couple by the long-range dipolar interaction, giving rise to chiral transport phenomena [9–11].

Strong coherent coupling between photons in high-quality cavities and spin ensembles such as nitrogen-vacancy centers in diamond [12,13], rare-earth ions [14,15], and ferromagnets [16–19] is attractive because of its potential for quantum memories [20] and transducers. While a (nearly) closed cavity can have very long photon lifetimes, efficient photon transport requires an open waveguide, which is the main object of the present study. Coherent microwave emission from a precessing magnetization of a ferromagnet in a waveguide can be measured via the additional damping of magnons [21–25] on top of the intrinsic Gilbert damping. The Larmor precession of the magnetization couples preferentially to photons with the same polarization. Due to the tunable ellipticity of the AC magnetic field, magnets at certain locations in a waveguide also couple preferentially to photons propagating in one direction. Such a chiral coupling [26] of atoms and quantum dots with optical photons attracts much attention [27–32]. Microwave devices such as nonreciprocal band rejection filters operate by placing a ferromagnet on special points in waveguides with circular polarization [33–35].

Here we study a collection of magnetic particles placed in a microwave waveguide [23,36,37], as shown in Fig. 1. The radiation emitted by a magnet typically drives all the other magnets, leading to an effective long-range dissipative coupling, reminiscent of—but very different from—the coherent coupling in a closed cavity [20,38]. The coupling mediated by traveling photons in atomic ensembles [39–44] causes collective super- and subradiance. Here, we discuss analogous modes in macroscopic magnonic systems but incorporating the chirality, which can be probed by microwaves at room temperature.

We show that magnets can couple chirally to waveguide photons, leading to nonreciprocal magnon-magnon interaction [27]. For given locations in a waveguide, one magnet can affect another one without back action [32]. We predict an imbalance of the magnon population in two spheres of up to one order of magnitude, which can be significantly enhanced in a chain of magnets. We study the collective excitations of up to $\sim$100 magnets, focusing on superradiant and subradiant modes, i.e., modes with very high or low radiation efficiency. We find that the superradiant states [39–43] are well localized at the edge of the chain [39,45]. In contrast, the lowest subradiant states are standing-wave-like and centered in the chain and are only weakly affected by the chirality of the coupling. In the accompanying letter [46], we introduce this effect and focus on the functionality of generating very large magnon amplitudes at the edges of magnetic chains in a waveguide and work out its enhancement by chirality. Here we formulate the theory and observables for the physical properties of the collective modes for one, two, and many spheres in a waveguide, such as the microwave transmission spectra.

This paper is organized as follows. We introduce the model in Sec. II, including the Hamiltonian and photon scattering matrix for a general waveguide geometry and positions of the magnets. After a focus on magnon-photon coupling in a rectangular waveguide in Sec. III, we address the radiative damping of magnets in Sec. IV. In Sec. V, we discuss the transmission of a waveguide with two magnetic spheres, introducing the concept of imbalanced pumping. We derive collective modes with super- and subradiance in long magnetic chains in Sec. VI. Finally, Sec. VII contains a discussion of the results and conclusions.

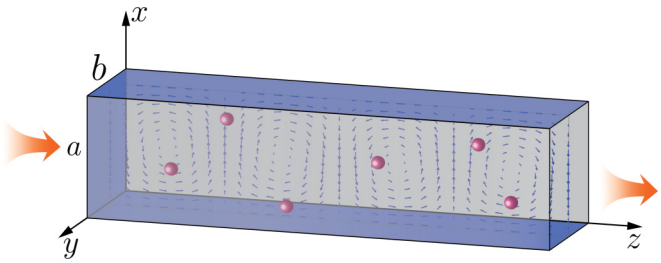

FIG. 1. An ensemble of magnets in a waveguide along the z direction. The input photon shown by the red arrow experiences scattering by magnets and its transmission can be used to detect the magnon dynamics.

II. MODEL

We focus here on magnets that are small enough compared with the photon wavelength such that only the homogeneous collective excitation or Kittel mode couples with the microwave photon [47,48]. We consider a waveguide infinite in the **z** direction with a rectangular cross section from (0,0) to (a, b), as shown in Fig. 1. We assume metallic boundaries, i.e., the electric field parallel to the surface vanishes. There are N equivalent magnets with gyromagnetic ratio $-\tilde{\gamma}$, saturation magnetization M_s, and volume V_s . Their centers are at $\mathbf{r}_i = (\boldsymbol{\rho}_i, z_i)$, where $\boldsymbol{\rho} = (x, y)$ is the position in the waveguide's cross section.

The dynamics is governed by the Hamiltonian $\hat{H} = \hat{H}_{\rm em} + \hat{H}_{\rm m} + \hat{H}_{\rm int}$, with electromagnetic contribution

$$\hat{H}_{\rm em} = \int \left[\frac{\epsilon_0}{2}\mathbf{E}(\mathbf{r})\cdot\mathbf{E}(\mathbf{r}) + \frac{\mu_0}{2}\mathbf{H}(\mathbf{r})\cdot\mathbf{H}(\mathbf{r})\right]d\mathbf{r}, \quad (1)$$

the magnetic part

$$\hat{H}_{\rm m} = -\mu_0 \int [H_{\rm app}(\mathbf{r})M_y(\mathbf{r}) + \mathbf{H}_{\rm eff}(\mathbf{r})\cdot\mathbf{M}(\mathbf{r})]d\mathbf{r}, \quad (2)$$

and the magnon-photon interaction

$$\hat{H}_{\rm int} = -\mu_0 \int \mathbf{H}(\mathbf{r})\cdot\mathbf{M}(\mathbf{r})d\mathbf{r}. \quad (3)$$

The time dependence is implicit. Here, $\{\mathbf{E}, \mathbf{H}\}$ represent the electric and magnetic fields of the photons in the waveguide, $\mathbf{H}_{\rm eff}(\mathbf{r})$ is the sum of dipolar and exchange interaction [49], $\mathbf{M}$ is the magnetization, ϵ_0 and μ_0 are the permittivity and permeability of the free space, and $H_{\rm app}(\mathbf{r})$ is the modulus of the static applied field along y that saturates the magnetizations.

The Hamiltonian gives the Maxwell equations [26],

$$\begin{aligned} \nabla\times\mathbf{E} = -\mu_0\frac{\partial\mathbf{H}}{\partial t},\quad \nabla\times\mathbf{H} = \epsilon_0\frac{\partial\mathbf{E}}{\partial t},\\ \nabla\cdot\mathbf{H} = -\nabla\cdot\mathbf{M},\quad \nabla\cdot\mathbf{E} = 0, \end{aligned} \quad (4)$$

and the Landau-Lifshitz equation [49]

$$\frac{\partial\mathbf{M}}{\partial t} = -\tilde{\gamma}\mu_0\mathbf{M}\times(\mathbf{H} + \mathbf{H}_{\rm eff} + H_{\rm app}\mathbf{y}). \quad (5)$$

The electromagnetic fields can be expanded in photon operators,

$$\mathbf{H}(\mathbf{r}) = \sum_\lambda \int_{-\infty}^{\infty} \left(\boldsymbol{\mathscr{H}}_k^{(\lambda)}(\boldsymbol{\rho})e^{ikz}\hat{p}_k^{(\lambda)} + \text{H.c.}\right)\frac{dk}{\sqrt{2\pi}}, \quad (6)$$

with $\boldsymbol{\mathscr{H}}_k^{(\lambda)}(\boldsymbol{\rho})$ being the eigenmodes for the magnetic field in the waveguide [26], and similarly for the electric field with $\mathbf{H}\to\mathbf{E}$ and $\boldsymbol{\mathscr{H}}\to\boldsymbol{\mathscr{E}}$. Here k denotes the momentum in the **z** direction, and λ represents the mode structure (including the polarization). The photon operators satisfy the field commutation relations

$$\left[\hat{p}_k^{(\lambda)}, \hat{p}_{k'}^{(\lambda)'\dagger}\right] = \delta(k-k')\delta_{\lambda\lambda'}. \quad (7)$$

The Cartesian components of the eigenmodes $\boldsymbol{\mathscr{H}}_k^{(\lambda)}(\rho)$ and $\boldsymbol{\mathscr{E}}_{\boldsymbol{k}}^{(\lambda)}(\boldsymbol{\rho})$ in a waveguide satisfy the orthonormality relations [26],

$$\begin{aligned} &\int \left(\mathscr{H}_{k,x}^{(\lambda)*}\mathscr{H}_{k,x}^{(\lambda')} + \mathscr{H}_{k,y}^{(\lambda)*}\mathscr{H}_{k,y}^{(\lambda')}\right)d\boldsymbol{\rho} = \frac{A_k^{(\lambda)}}{\left(Z_k^{(\lambda)}\right)^2}\delta_{\lambda\lambda'},\\ &\int \mathscr{H}_{k,z}^{(\lambda)*}\mathscr{H}_{k,z}^{(\lambda')}d\boldsymbol{\rho} = \frac{\gamma_\lambda^2 A_k^{(\lambda)}}{k^2\left(Z_k^{(\lambda)}\right)^2}\delta_{\lambda\lambda'} \quad \text{(TE)},\\ &\int \left(\mathscr{E}_{k,x}^{(\lambda)*}\mathscr{E}_{k,x}^{(\lambda')} + \mathscr{E}_{k,y}^{(\lambda)*}\mathscr{E}_{k,y}^{(\lambda')}\right)d\boldsymbol{\rho} = A_k^{(\lambda)}\delta_{\lambda\lambda'},\\ &\int \mathscr{E}_{k,z}^{(\lambda)*}\mathscr{E}_{k,z}^{(\lambda')}d\boldsymbol{\rho} = \frac{\gamma_\lambda^2 A_k^{(\lambda)}}{k^2}\delta_{\lambda\lambda'}, \quad \text{(TM)}. \end{aligned} \quad (8)$$

Here, $Z_k^{(\lambda)} = \mu_0\Omega_k^{(\lambda)}/k$ and $k/(\epsilon_0\Omega_k^{(\lambda)})$ are, respectively, the impedances for the TE and TM modes [26], $A_k^{(\lambda)} = \hbar\Omega_k^{(\lambda)}/(2\epsilon_0)$ and $\hbar/(2\epsilon_0\Omega_k^{(\lambda)})$ for the TE and TM modes with $\Omega_k^{(\lambda)}$ being the eigenfrequency and

$$\gamma_\lambda^2 = \left(\Omega_k^{(\lambda)}\right)^2/c^2 - k^2. \quad (9)$$

TE (TM), i.e., transverse electric (magnetic) polarization, refers to the case when the electric (magnetic) field is perpendicular to the **z** direction. It is noted that these normalizations are chosen such that the Hamiltonian Eq. (1) satisfies (up to a constant)

$$\hat{H}_{\rm em} = \sum_\lambda \int \hbar\Omega_k^{(\lambda)}\hat{p}_k^{(\lambda)\dagger}\hat{p}_k^{(\lambda)}dk. \quad (10)$$

We assume the losses in high-quality waveguides to be small compared to the magnetic dissipation and not important on the length scale of interest.

The magnetization $\mathbf{M}(\mathbf{r})$ is confined to the magnets that are much smaller than typical photon wavelengths and waveguide dimensions (usually >1 cm), such that the magnetic field is a constant inside each magnet. The excitations of the (linearized) magnetic Hamiltonian are spin waves, or its quanta, magnons. For magnets with axial symmetry around the magnetization, the microwaves couple strongly only with the Kittel mode, i.e., the uniform precession of the magnetization, and we disregard other modes in the following. We quantize the magnetization as [50–52]

$$\begin{aligned} M_{j,z} - iM_{j,x} &= \sqrt{\frac{2\hbar\tilde{\gamma}M_s}{V_s}}\hat{m}_j,\\ M_{j,y} &= M_s - \frac{\hbar\tilde{\gamma}}{V_s}\hat{m}_j^\dagger\hat{m}_j, \end{aligned} \quad (11)$$

where $\hat{m}_j$ is the annihilation operator for a Kittel magnon in the jth magnet with $j\in\{1,\ldots,N\}$. The coefficients are

chosen to ensure that $\mathbf{M}_j \cdot \mathbf{M}_j \approx M_s^2$ and the magnetic Hamiltonian Eq. (2), up to a constant due to zero-point fluctuations, becomes

$$\hat{H}_{\rm m} = \sum_{j=1}^{N} \hbar\omega_j \hat{m}_j^\dagger \hat{m}_j, \tag{12}$$

where $\omega_j = \tilde{\gamma}\mu_0[H_{\rm app}(\mathbf{r}_j) + H_{\rm eff}(\mathbf{r}_j)]$ with $H_{\rm eff} = N_y H_{\rm app}$ for axially symmetric magnets (N_y is the demagnetization factor).

Inserting Eqs. (6) and (11) into the interaction Hamiltonian Eq. (3),

$$\hat{H}_{\rm int} = \sum_{j\lambda} \int \left[\hbar g_j^{(\lambda)}(k)\hat{p}_k^{(\lambda)}\hat{m}_j^\dagger + {\rm H.c.}\right]\frac{dk}{\sqrt{2\pi}}, \tag{13}$$

with coupling constant

$$g_j^{(\lambda)}(k) = \mu_0\sqrt{\frac{\tilde{\gamma}M_s V_s}{2\hbar}}e^{ikz_j}\left[i\mathscr{H}_{k,x}^{(\lambda)}(\boldsymbol{\rho}_j) - \mathscr{H}_{k,z}^{(\lambda)}(\boldsymbol{\rho}_j)\right]. \tag{14}$$

The distributed magnets experience different phases when their distance is not much smaller than the photon wavelength. We can tune coupling strength and chirality by the position of the magnets $\boldsymbol{\rho}_j$, see Sec. III.

The effective fields should in principle be computed self-consistently, since a magnetic sphere can be a significant perturbation of the electric and magnetic microwave fields [53]. This problem can be solved semianalytically by Mie theory in special situations [38]. The hinges and local sources that address individual spheres also cause interferences that must be addressed numerically [54]. With the knowledge that the results will not change qualitatively, we use here a perturbative approach, by assuming that the driving fields are those of the unperturbed system.

A. Equations of motion

From the Hamiltonian $\hat{H} = \hat{H}_{\rm em} + \hat{H}_{\rm m} + \hat{H}_{\rm int}$, we obtain the equation of motion for photons by the Heisenberg equation

$$\frac{d\hat{p}_k^{(\lambda)}}{dt} = -i\Omega_k^{(\lambda)}\hat{p}_k^{(\lambda)} - i\sum_j \frac{g_j^{(\lambda)*}(k)}{\sqrt{2\pi}}\hat{m}_j. \tag{15}$$

The solutions are

$$\hat{p}_k^{(\lambda)}(t) = \hat{p}_{k,{\rm in}}^{(\lambda)}e^{-i\Omega_k^{(\lambda)}t} - \sum_j \frac{ig_j^{(\lambda)*}(k)}{\sqrt{2\pi}}\int_{-\infty}^{t}\hat{m}_j(\tau)e^{-i\Omega_k^{(\lambda)}(t-\tau)}d\tau, \tag{16}$$

where $\hat{p}_k(-\infty) \equiv \hat{p}_{k,{\rm in}}^{(\lambda)}$ is the microwave input [55,56]. The first term is the free evolution and the second term is the (spontaneous and stimulated) radiation generated by magnons. The output field $\hat{p}_{k,{\rm out}}^{(\lambda)} = \lim_{t\to\infty}\hat{p}_k^{(\lambda)}(t)e^{i\Omega_k^{(\lambda)}t}$ then reads

$$\hat{p}_{k,{\rm out}}^{(\lambda)} = \hat{p}_{k,{\rm in}}^{(\lambda)} - i\sum_j \frac{g_j^{(\lambda)*}(k)}{\sqrt{2\pi}}\int_{-\infty}^{\infty} d\tau\ \hat{m}_j(\tau)e^{i\Omega_k^{(\lambda)}\tau}. \tag{17}$$

The magnon dynamics is governed by equation of motion

$$\frac{d\hat{m}_j}{dt} = -i\omega_j\hat{m}_j - \hat{\mathscr{D}}_{{\rm int},j} - \hat{\mathscr{D}}_{{\rm ph},j}, \tag{18}$$

where

$$\hat{\mathscr{D}}_{{\rm int},j} = \frac{\kappa_j}{2}\hat{m}_j + \sqrt{\kappa_j}\hat{N}_j, \tag{19}$$

$$\hat{\mathscr{D}}_{{\rm ph},j} = i\sum_\lambda \int \frac{dk}{\sqrt{2\pi}}g_j^{(\lambda)}(k)\hat{p}_k^{(\lambda)}, \tag{20}$$

equivalent to the linearized Landau-Lifshitz-Gilbert (LLG) equation. Here the linewidth $\kappa_j = 2\alpha_G\omega_j$, where α_G is the Gilbert damping parameter. Each magnet j is connected to an intrinsic bath of phonons and other magnons, which generates the thermal torque $\hat{\mathscr{D}}_{{\rm int},j}$. We model this interaction by a Markovian processes with intrinsic linewidth κ_j and white noise $\hat{N}_j$ satisfying $\langle\hat{N}_j\rangle = 0$, $\langle\hat{N}_j^\dagger(t)\hat{N}_j(t')\rangle = n_j\delta(t-t')$ and $\langle\hat{N}_j(t)\hat{N}_j^\dagger(t')\rangle = (n_j+1)\delta(t-t')$, where

$$n_j = \left[\exp\left(\frac{\hbar\omega_j}{k_B T}\right) - 1\right]^{-1} \tag{21}$$

is the thermal occupation of magnons at a global temperature T. In the absence of coupling between different magnets by a waveguide, $\hat{\mathscr{D}}_{{\rm ph},j} = 0$ and all magnons are Gibbs distributed at equilibrium [55].

When magnons are coupled by photons, the torque $\hat{\mathscr{D}}_{{\rm ph},j}$ can be split as

$$\hat{\mathscr{D}}_{{\rm ph},j}(t) = \hat{T}_j(t) + i\sum_l \int_{-\infty}^{t} d\tau\ \tilde{\Sigma}_{jl}(t-\tau)\hat{m}_l(\tau), \tag{22}$$

where the first term is generated by the photon input,

$$\hat{T}_j(t) = i\sum_\lambda \int \frac{dk}{\sqrt{2\pi}}g_j^{(\lambda)}(k)\hat{p}_{k,{\rm in}}^{(\lambda)}e^{-i\Omega_k^{(\lambda)}t}, \tag{23}$$

while the second term describes the photon-mediated coupling

$$\tilde{\Sigma}_{jl}(t-\tau) = -i\sum_\lambda \int \frac{dk}{2\pi}g_j^{(\lambda)}(k)g_l^{(\lambda)*}(k)e^{-i\Omega_k^{(\lambda)}(t-\tau)}, \tag{24}$$

which can be interpreted as (real or virtual) (λ, k)-mode photon emission from magnet l with amplitude $g_l^{(\lambda)*}(k)$ followed by absorption in magnet j with amplitude $g_j^{(\lambda)}(k)$. The interaction is retarded by the finite light velocity. However, even for large distances $r_{jl} < 1\,{\rm m}$, $\kappa_j r_{jl}/c < 0.02$, where $\kappa_j = 2\pi \times 1\,{\rm MHz}$ is a typical magnon linewidth, so $\tilde{\Sigma}_{jl}(t-\tau)$ decays much faster than the magnon envelope dynamics. For short times $|t-\tau| < r_{jl}/c$, the magnons may be assumed to move coherently $\hat{m}_l(\tau) \approx \hat{m}_l(t)e^{i\omega_l(t-\tau)}$. This adiabatic approximation simplifies Eq. (18) to

$$\frac{d\hat{\mathscr{M}}}{dt} = -i\tilde{\omega}\hat{\mathscr{M}} - i\Sigma\hat{\mathscr{M}} - \hat{\mathscr{T}} - \hat{\mathscr{N}}, \tag{25}$$

introducing the column vectors for magnetization $\hat{\mathscr{M}} = (\hat{m}_1, \ldots, \hat{m}_N)^T$, the noise

$$\hat{\mathscr{N}} = (\sqrt{\kappa_1}\hat{N}_1, \cdots, \sqrt{\kappa_N}\hat{N}_N)^T, \tag{26}$$

and the (microwave) torque

$$\hat{\mathscr{T}} \equiv (\hat{T}_1, \cdots, \hat{T}_N)^T = i\sum_\lambda \int \hat{p}_{k,{\rm in}}^{(\lambda)}e^{-i\Omega_k^{(\lambda)}t}\mathscr{G}_k^{(\lambda)}\frac{dk}{\sqrt{2\pi}}, \tag{27}$$

with coupling $\mathscr{G}_k^{(\lambda)} = (g_1^{(\lambda)}(k), \ldots, g_N^{(\lambda)}(k))^T$. A local antenna such as metal-wire coils close to each sphere [20] can locally excite or detect its dynamics, leading to the distributed torque $\hat{\mathscr{T}} \to \hat{\mathscr{T}} + \hat{\mathscr{T}}_l$, where $\hat{\mathscr{T}}_l = (\hat{P}_1, \cdots, \hat{P}_N)^T$ and $\hat{P}_i$ is the local input amplitude. The elements of the matrices $\tilde{\omega}$ and Σ read

$$\tilde{\omega}_{jl} = \delta_{jl}\left(\omega_j - i\frac{\kappa_j}{2}\right), \tag{28}$$

$$\Sigma_{jl} = \int_0^\infty \tilde{\Sigma}_{jl}(t) e^{i\omega_l t} dt. \tag{29}$$

Inserting $\tilde{\Sigma}$, we obtain the self-energy

$$\Sigma_{jl} = \sum_\lambda \int \frac{dk}{2\pi} \frac{g_j^{(\lambda)}(k) g_l^{(\lambda)*}(k)}{\omega_l - \Omega_k^{(\lambda)} + i0^+}. \tag{30}$$

According to Eq. (25), $\mathrm{Re}\Sigma$ modulates the frequencies of each magnon by the other magnons (coherent coupling), while $\mathrm{Im}\Sigma$ changes the damping (dissipative coupling). We discuss Σ in more detail for a rectangular waveguide below.

B. Collective modes

The coupling between magnets by photon exchange in the waveguide gives rise to collective excitations. In the language of quantum optics [39–43,55,57,58], Eq. (25) can be interpreted as a non-Hermitian Hamiltonian, $\hat{H}_{\mathrm{eff}} = \hbar \hat{\mathscr{M}}^\dagger \tilde{H}_{\mathrm{eff}} \hat{\mathscr{M}}$, with matrix

$$\tilde{H}_{\mathrm{eff}} = (\tilde{\omega} + \Sigma), \tag{31}$$

which (without input $\hat{\mathscr{T}}$) recovers the Heisenberg equation [39–43,57]. Master equations lead to an effective non-Hermitian Hamiltonian by exploiting the Monte Carlo wave-function method in quantum optics [57]. In general, any two systems coupled via continuous traveling waves are dissipatively coupled.

The right and left eigenvectors of the non-Hermitian $\tilde{H}_{\mathrm{eff}}$ are not the same. Let the right eigenvectors of $\tilde{H}_{\mathrm{eff}}$ be $\{\psi_\zeta\}$ with corresponding eigenvalues $\{\nu_\zeta\}$ where $\zeta \in \{1, \ldots, N\}$ label the collective modes. It is also convenient to define the right eigenvectors of $\tilde{H}_{\mathrm{eff}}^\dagger$ as $\{\phi_\zeta\}$ with corresponding eigenvalues $\{\nu_\zeta^*\}$. Without degeneracies, i.e., $\forall_{\zeta\zeta'}\ \nu_\zeta \neq \nu_{\zeta'}$, we have biorthonormality $\psi_\zeta^\dagger \phi_{\zeta'} = \delta_{\zeta\zeta'}$ after normalization. $\phi_\zeta^\dagger$ is a left eigenvector of $\tilde{H}_{\mathrm{eff}}$. The nonuniqueness of the normalization condition does not affect the observables.

Defining matrices $\mathscr{L} = (\phi_1, \ldots, \phi_N)$ and $\mathscr{R} = (\psi_1, \ldots, \psi_N)$ in terms of left and right eigenvectors, biorthonormality $\mathscr{R}^\dagger \mathscr{L} = \mathscr{L}^\dagger \mathscr{R} = I_N$, where I_N is the $N \times N$ identity matrix, leads to

$$\tilde{\omega} + \Sigma = \mathscr{R} \nu \mathscr{L}^\dagger, \tag{32}$$

with matrix elements $\nu_{ij} = (\nu_1, \ldots, \nu_N)\delta_{ij}$. Defining

$$\hat{\alpha}_\zeta = \phi_\zeta^\dagger \hat{\mathscr{M}}, \tag{33}$$

$\hat{\alpha}_\zeta$ annihilates a quasiparticle in a collective mode with "wave function" ψ_ζ. Substituting Eq. (32) into Eq. (25) leads to the equation of motion

$$\frac{d\hat{\alpha}_\zeta}{dt} = -i\nu_\zeta \hat{\alpha}_\zeta - \hat{\tau}_\zeta - \hat{N}_\zeta, \tag{34}$$

where

$$\hat{\tau}_\zeta = \phi_\zeta^\dagger \hat{\mathscr{T}};\ \ \hat{N}_\zeta = \phi_\zeta^\dagger \hat{\mathscr{N}}. \tag{35}$$

The magnetization follows from the right eigenvectors:

$$\hat{\mathscr{M}}(t) = \sum_\zeta \hat{\alpha}_\zeta(t) \psi_\zeta. \tag{36}$$

C. Photon scattering matrix

The coupled set of magnets leads to collective excitations that affect the transmission and reflection of input photons with frequency ω_{in}. The ensemble average $\langle \cdots \rangle$ of input mode λ is

$$\langle \hat{p}_{k,\mathrm{in}}^{(\lambda)} \rangle = \sqrt{2\pi} A_\lambda \delta(k - k_\lambda), \tag{37}$$

where A_λ is the amplitudes of the incoming microwave field and k_λ is the positive wave vector satisfying $\Omega_{k_\lambda}^{(\lambda)} = \omega_{\mathrm{in}}$. $\Omega_k^{(\lambda)} = \Omega_{-k}^{(\lambda)}$ and we assume that k_λ is unique, which is satisfied in the absence of spatial modulations. The average of the torque Eq. (35) acting on mode ζ:

$$\langle \hat{\tau}_\zeta \rangle = i \sum_\lambda A_\lambda e^{-i\omega_{\mathrm{in}} t} \mathscr{A}_{\zeta+}^{(\lambda)}. \tag{38}$$

The absorption coefficients,

$$\mathscr{A}_{\zeta\pm}^{(\lambda)} \equiv \phi_\zeta^\dagger \mathscr{G}_{\pm k_\lambda}^{(\lambda)}, \tag{39}$$

are a linear combination of $g_j^{(\lambda)}$'s with weights given by the left eigenvector. We argue below that the latter may be localized to only a few magnets, such that a local coupling constant can dominate the global absorption.

The average amplitude of mode ζ follows from Eq. (34). In the steady state,

$$\langle \hat{\alpha}_\zeta(t) \rangle = \sum_\lambda A_\lambda e^{-i\omega_{\mathrm{in}} t} \frac{\mathscr{A}_{\zeta+}^{(\lambda)}}{\omega_{\mathrm{in}} - \nu_\zeta}. \tag{40}$$

Mode ζ is resonantly excited when $\omega_{\mathrm{in}} = \mathrm{Re}\nu_\zeta$ with spectral broadening $\mathrm{Im}\nu_\zeta$. The photon output Eq. (17) is

$$\langle \hat{p}_{k,\mathrm{out}}^{(\lambda)} \rangle = \langle \hat{p}_{k,\mathrm{in}}^{(\lambda)} \rangle - i \sum_\zeta \mathscr{E}_{\zeta\pm}^{(\lambda)} \int \hat{\alpha}_\zeta(\tau) e^{i\Omega_k^{(\lambda)}\tau} \frac{d\tau}{\sqrt{2\pi}}, \tag{41}$$

with + (-) sign for $k > 0$ ($k < 0$), while the emission coefficient

$$\mathscr{E}_{\zeta\pm}^{(\lambda)} \equiv \mathscr{G}_{\pm k_\lambda}^{(\lambda)\dagger} \psi_\zeta \tag{42}$$

is a linear combination of couplings $g_j^{(\lambda)}$ weighted by the right eigenvector. When the latter is localized, emission is governed by a few magnetic moments and couplings between them.

The coherent output,

$$\langle \hat{p}_{k,\mathrm{out}}^{(\lambda)} \rangle = \sqrt{2\pi} \sum_{\lambda'} [S_{12}^{(\lambda\lambda')} \delta(k - k_\lambda) + S_{22}^{(\lambda\lambda')} \delta(k + k_\lambda)] A_{\lambda'}, \tag{43}$$

contains a transmission

$$S_{12}^{(\lambda\lambda')}(\omega_{\mathrm{in}}) = \delta_{\lambda\lambda'} - \frac{i}{v^{(\lambda)}(k_\lambda)} \sum_{\zeta=1}^N \frac{\mathscr{E}_{\zeta+}^{(\lambda)} \mathscr{A}_{\zeta+}^{(\lambda')}}{\omega_{\mathrm{in}} - \nu_\zeta} \tag{44}$$

and a reflection amplitude

$$S_{11}^{(\lambda\lambda')}(\omega_{\rm in}) = -\frac{i}{v^{(\lambda)}(k_\lambda)} \sum_{\zeta=1}^{N} \frac{\mathscr{E}_{\zeta-}^{(\lambda)} \mathscr{A}_{\zeta+}^{(\lambda')}}{\omega_{\rm in} - \nu_\zeta}, \tag{45}$$

with photon group velocity

$$v^{(\lambda)}(k) = \left| d\Omega_k^{(\lambda)} / dk \right|. \tag{46}$$

S_{21} and S_{22} can be found, respectively, from S_{11} and S_{12} by the substitution $\mathscr{A}_{\zeta+}^{(\lambda)} \to \mathscr{A}_{\zeta-}^{(\lambda)}$. The (interband) scattering amplitudes resonate at N eigenfrequencies of the collective magnetic modes.

This result can be derived as well from scattering theory [59–62].

III. RECTANGULAR WAVEGUIDE

We discuss here the coupling matrix Σ for a rectangular waveguide with a cross section from (0,0) to $(a \geqslant b, b)$, with a detailed derivation in Appendix A. We use transverse mode indices $\lambda \equiv \{n_x, n_y, \sigma\}$, in which integers $n_x, n_y \geqslant 0$ are the number of nodes of magnetic (or electric) field in the **x** and **y** directions, and $\sigma \in \{\text{TE}, \text{TM}\}$ denotes the polarization. The photon dispersion is [26]

$$\Omega_k^{(\lambda)} = c\sqrt{k^2 + \gamma_\lambda^2}, \tag{47}$$

where $\gamma_\lambda \equiv \sqrt{(\gamma_x^{(\lambda)})^2 + (\gamma_y^{(\lambda)})^2}$ with $\gamma_x^{(\lambda)} = \pi n_x/a$ and $\gamma_y^{(\lambda)} = \pi n_y/b$, does not depend on polarization index σ.

The diagonal elements of the coupling Σ_{jj} in Eq. (30) represent self-interaction that shifts the frequencies by a small amount ($\text{Re}\,\Sigma_{jj} \ll \omega_j$ as shown below) and describe the radiative damping $\text{Im}\,\Sigma_{jj}$, see Sec. IV. The nondiagonal elements $\Sigma_{i\neq l}$ couple different magnets. With $\tilde{g}_j^{(\lambda)}(k) = -ig_j^{(\lambda)}(k)e^{-ikz_j}$, where $\text{Im}\tilde{g}_j^{(\lambda)}(k) = 0$ (see Appendix A), we obtain an effective coupling

$$\Sigma_{jl} = \sum_{\lambda}^{\text{Im}k_l^{(\lambda)}=0} \begin{cases} -i\frac{\Gamma_L+\Gamma_R}{2} - \delta\omega_j^{(\lambda)}, & j = l \\ -i\Gamma_R e^{ik_l^{(\lambda)}(z_j - z_l)}, & z_j > z_l \\ -i\Gamma_L e^{ik_l^{(\lambda)}(z_l - z_j)}, & z_j < z_l, \end{cases} \tag{48}$$

that is modulated by geometric phase factors. As discussed in Appendix A in more detail, the contribution from evanescent fields generated by nonresonant higher-frequency cavity modes is disregarded, which is allowed when $|k_l^{(\lambda)}||z_j - z_l| \gtrsim 1$. With waveguide cross sections of the order of centimeters, the magnets should be separated by at least a few millimeters.

Here, the frequency shift for magnet j by the photon band λ reads

$$\delta\omega_j^{(\lambda)} = \frac{\gamma\mu_0 M_s V_s k_c}{ab} \sin^2\left(\gamma_x^{(\lambda)} x_j\right) \cos^2\left(\gamma_y^{(\lambda)} y_j\right), \tag{49}$$

where k_c is an upper cutoff for the wave numbers, which is typically governed by high-frequency losses in the boundaries. For typical electron relaxation time in copper, $\tau_{\rm el} = 50\,\text{fs}$ ($\Omega_c \sim 2\pi \times 20\,\text{THz}$) [63], $k_c = 2\pi/(\tau_{\rm el} c) \sim 10^5\ \text{m}^{-1}$, and $\delta\omega_j^{(\lambda)} \lesssim 2\pi \times 100\,\text{MHz}$ for $a \sim b \sim 2\,\text{cm}$ and the sphere radius of 0.5 mm, which is much smaller than the Kittel mode frequency $\omega_j \sim 2\pi \times 10\,\text{GHz}$. The intermagnet coupling (suppressing various indices)

$$\Gamma_R = \frac{\tilde{g}_j^{(\lambda)}\left(k_l^{(\lambda)}\right)\tilde{g}_l^{(\lambda)}\left(k_l^{(\lambda)}\right)}{v^{(\lambda)}\left(k_l^{(\lambda)}\right)}, \tag{50}$$

with group velocity Eq. (46)

$$v^{(\lambda)}(k) = c^2|k|/\Omega_k^{(\lambda)}, \tag{51}$$

and (positive) wave number of the photons emitted by the lth magnet is

$$k_l^{(\lambda)} = \sqrt{\omega_l^2/c^2 - \gamma_\lambda^2}. \tag{52}$$

The summation in Eq. (48) is limited over the λ's for which $k_l^{(\lambda)}$ is real, i.e., the frequency of the lth magnet is larger than the λ-band edge. Γ_L is obtained from Γ_R by $k_l^{(\lambda)} \to -k_l^{(\lambda)}$.

For our rectangular waveguide, the couplings between magnets mediated by the TM and TE photons are

$$\tilde{g}_j^{(\lambda)}\left(\pm k_l^{(\lambda)}\right)|_{\rm TM} = G_l \frac{\gamma_y^{(\lambda)}}{\gamma_\lambda} \sin\left(\gamma_x^{(\lambda)} x_j\right) \cos\left(\gamma_y^{(\lambda)} y_j\right) \tag{53}$$

and

$$\tilde{g}_j^{(\lambda)}(\pm k_l^{(\lambda)})|_{\rm TE} = G_l \frac{c k_l^{(\lambda)}}{\omega_j} \frac{\gamma_x^{(\lambda)}}{\gamma_\lambda} \cos\left(\gamma_y^{(\lambda)} y_j\right) \times \left[-\sin\left(\gamma_x^{(\lambda)} x_j\right) \pm \frac{\gamma_\lambda^2}{k_l^{(\lambda)} \gamma_x^{(\lambda)}} \cos\left(\gamma_x^{(\lambda)} x_j\right) \right], \tag{54}$$

respectively, where

$$G_l = \sqrt{\frac{\tilde{\gamma}\mu_0 M_s V_s \omega_l}{ab}}. \tag{55}$$

For the TE modes, the magnon-photon coupling depends on the direction of propagation. The chirality $\tilde{g}_j^{(\lambda)}(k_l^{(\lambda)})|_{\rm TE} \neq \tilde{g}_j^{(\lambda)}(-k_l^{(\lambda)})|_{\rm TE}$ is caused by a magnetic field that is not linearly polarized, as indicated for the $\{n_x = 1, n_y = 0\}$ mode in Fig. 2. When $z_j > z_l$ and the jth magnet is located at a position x_j, satisfying

$$\cot\left(\frac{\pi x_j}{a}\right) = -\sqrt{\frac{a^2\omega_l^2}{\pi^2 c^2} - 1}, \tag{56}$$

the magnon-photon coupling is fully chiral $\Sigma_{jl} = 0$, so the lth magnet does not affect the jth one. The coupling is also nonreciprocal, i.e., one magnet feels the dynamics of another, but not the other way around.

When tuning the magnon frequency to below the bottom of all λ bands except for the lowest TE_{10} mode (the TE_{00} mode does not exist), i.e.,

$$\frac{\pi}{a} < \frac{\omega_l}{c} < \left\{\frac{\pi}{b}, \frac{2\pi}{a}\right\}, \tag{57}$$

we can freely tune the chirality. Figure 2 shows a snapshot of the magnetic field for the lowest TE_{10} mode propagating along the $-\mathbf{z}$ direction. For modes along the **z** direction, the local ellipticity is reversed. Solving Eq. (56) with $\omega_l = (2/\sqrt{3})c\pi/a$, magnon-photon coupling is fully chiral for magnets on the green and red dotted line. The chirality vanishes on the center

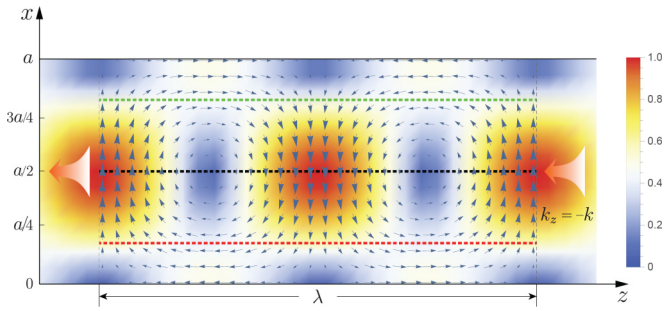

FIG. 2. Snapshot of the spatial distribution of the AC magnetic field of the lowest TE_{10} mode in a rectangular waveguide propagating along the $-z$ direction. The arrows indicate the direction and their lengths the modulus of the field. The latter is also indicated by the color shading, from zero (dark blue) to the maximum value (dark red). The vector field of modes in the opposite (not shown) is reversed. The green and red (black) dotted lines indicate the locations at which the magnon-photon coupling is chiral (nonchiral) for magnon frequency tuned to $\omega_l = (2/\sqrt{3})c\pi/a$. On the red (green) line, the magnon mode only couples to photons with positive (negative) linear momentum.

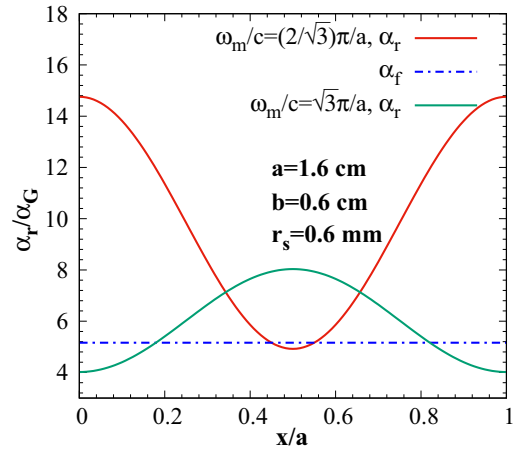

FIG. 3. Position-dependent radiative damping α_r scaled by the intrinsic Gilbert damping α_G of a YIG sphere by the TE_{10} mode of a rectangular waveguide for two magnetic frequencies ω_m. The parameters including a are specified in the text. The free space radiative damping α_f from Appendix B is also given (for the larger $\omega_m = (2/\sqrt{3})c\pi/a$).

(black dotted) line and is partially chiral everywhere else. Spectral overlap with TM photons at higher frequencies would reduce the chirality.

IV. MICROWAVE EMISSION BY MAGNETIZATION DYNAMICS

Analogous to the spin pumping [7,8,64], the transfer of energy and angular momentum from magnons to photons implies radiative damping. In a waveguide, this can be much larger than the intrinsic damping of a high-quality magnet such as YIG [21–23]. Radiative damping also exists in free space, as derived in Appendix B, but in the waveguide we can control its magnitude.

A. Radiative damping

In this section, we focus on a single magnet with (Kittel) frequency ω_m. The magnon lifetime broadening $\delta\omega = 2(\alpha_G + \alpha_r)\omega$, where α_G is the Gilbert damping parameter and [see Eq. (48)] [62,65–67]

$$\alpha_r = \frac{-\mathrm{Im}\Sigma}{\omega_m} = \sum_\lambda \frac{|g^{(\lambda)}(k^{(\lambda)})|^2 + |g^{(\lambda)}(-k^{(\lambda)})|^2}{2c^2 k^{(\lambda)}}, \tag{58}$$

where

$$k^{(\lambda)} = \sqrt{\frac{\omega_m^2}{c^2} - \left(\frac{\pi n_x}{a}\right)^2 - \left(\frac{\pi n_y}{b}\right)^2}. \tag{59}$$

We are mainly interested in the radiative damping of the lowest TE_{10} mode of a rectangular waveguide. The mode amplitude and the associated radiative damping do not depend on the y coordinate. Results are plotted in Fig. 3 for $\omega_m = (2/\sqrt{3})c\pi/a$, where $a = 1.6\,\mathrm{cm}$, $b = 0.6\,\mathrm{cm}$, a magnetic sphere with radius $r_s = 0.6\,\mathrm{mm}$ and intrinsic Gilbert damping $\alpha_G = 5 \times 10^{-5}$ [23] for two frequencies. α_r depends strongly on x, but weaker when close to the special position of chiral coupling, i.e., $x = a/3$ and $2a/3$ at $\omega_m = (2/\sqrt{3})c\pi/a$.

The radiative dissipation in the waveguide can be much larger than the viscous Gilbert damping as well as the radiative damping in free space [21], see Appendix B, Eq. (B7):

$$\alpha_f = \frac{\tilde{\gamma}\mu_0 M_s V_s \omega_m^2}{6\pi c^3}. \tag{60}$$

α_f scales like ω_m^2, and it can become larger than α_r at higher frequencies, because the photon density of states is suppressed by the waveguide.

The broadening of the ferromagnetic resonance is not so sensitive to g's chirality, but the transmission is. In the $\lambda = \{1, 0, \mathrm{TE}\}$ mode, the scattering matrix in Eqs. (44) and (45) reduces to

$$S_{12}(\omega_{\mathrm{in}}) = \frac{\omega_{\mathrm{in}} - \omega_m + i\alpha_G\omega_m + i(\Gamma_L - \Gamma_R)/2}{\omega_{\mathrm{in}} - \omega_m + i\alpha_G\omega_m + i(\Gamma_L + \Gamma_R)/2}, \tag{61}$$

where

$$\Gamma_R \equiv \frac{|g^{(\lambda)}(k^{(\lambda)})|^2}{v^{(\lambda)}(k^{(\lambda)})}, \quad \Gamma_L \equiv \frac{|g^{(\lambda)}(-k^{(\lambda)})|^2}{v^{(\lambda)}(k^{(\lambda)})}. \tag{62}$$

and $\alpha_r\omega_m = (\Gamma_L + \Gamma_R)/2$. When $\Gamma_L = \Gamma_R$, the transmission amplitude drops at the resonance $\omega_{\mathrm{in}} = \omega_m$ to a small value $\sim\alpha_G\omega_m/\Gamma_R$. However, for full chirality with $\Gamma_R = 0$, the magnet does not absorb photons traveling towards the right and the waveguide is transparent. When $\Gamma_L = 0$, on the other hand the transmission probability is still unity, but the phase is shifted by π.

B. Spatial chirality of dipolar field emission

The AC magnetic field in the waveguide emitted by a dynamical magnetic moment can be expressed by the linear response [8,64],

$$H_\alpha^r(\mathbf{r}, t) = -\mu_0 \int d\mathbf{r}' dt' \chi_{\alpha\beta}(\mathbf{r} - \mathbf{r}', t - t') M_\beta(\mathbf{r}', t'), \tag{63}$$

where the nonlocal inverse susceptibility $\chi_{\alpha\beta}$ is a correlation function of the photon magnetic field $\hat{\mathbf{H}}$:

$$\chi_{\alpha\beta}(\mathbf{r}-\mathbf{r}',t-t') = i\Theta(t-t')\langle[\hat{H}_\alpha(\mathbf{r},t),\hat{H}_\beta(\mathbf{r}',t')]\rangle. \quad (64)$$

For the present system,

$$\chi_{\alpha\beta}(\boldsymbol{\rho},z,\boldsymbol{\rho}',z';t-t') = i\Theta(t-t')\sum_\lambda \int \mathscr{H}^{(\lambda)}_{k,\alpha}(\boldsymbol{\rho})\mathscr{H}^{(\lambda)*}_{k,\beta}(\boldsymbol{\rho}') \times e^{ik(z-z')-i\Omega^{(\lambda)}_k(t-t')}\frac{dk}{2\pi}. \quad (65)$$

Disregarding the small damping, $M_\beta(\mathbf{r}',t') = M_\beta(\mathbf{r}')e^{i\omega_m(t-t')}$ and

$$H^r_\alpha(\mathbf{r},t) = \mu_0\sum_\lambda \int d\mathbf{r}' \int \frac{dk}{2\pi}\mathscr{H}^{(\lambda)}_{k,\alpha}(\boldsymbol{\rho})\mathscr{H}^{(\lambda)*}_{k,\beta}(\boldsymbol{\rho}') \times e^{ik(z-z')}\frac{1}{\omega_m-\Omega^{(\lambda)}_k+i0^+}M_\beta(\mathbf{r}',t). \quad (66)$$

This expression still includes the evanescent field by the sum over all (resonant and nonresonant) cavity modes. By contour integration over k for $z>z'$,

$$H^{r>}_\alpha(\mathbf{r},t) = -i\mu_0\sum_\lambda \frac{1}{v(k_\lambda)}\mathscr{H}^{(\lambda)}_{k_\lambda,\alpha}(\boldsymbol{\rho}) \times \int \mathscr{H}^{(\lambda)*}_{k_\lambda,\beta}(\boldsymbol{\rho}')M_\beta(\mathbf{r}',t)e^{ik_\lambda(z-z')}d\mathbf{r}', \quad (67)$$

and for $z<z'$,

$$H^{r<}_\alpha(\mathbf{r},t) = i\mu_0\sum_\lambda \frac{1}{v(k_\lambda)}\mathscr{H}^{(\lambda)}_{-k_\lambda,\alpha}(\boldsymbol{\rho}) \times \int \mathscr{H}^{(\lambda)*}_{-k_\lambda,\beta}(\boldsymbol{\rho}')M_\beta(\mathbf{r}',t)e^{-ik_\lambda(z-z')}d\mathbf{r}'. \quad (68)$$

We argue in the Appendices that the sum over distance modes can be disregarded since it causes only corrections very close to the magnet. Figure 4 illustrates the drastic effect of chirality by a snapshot of the emitted magnetic field (normalized to the maximum modulus and disregarding the evanescent wave corrections) by a magnet on a chiral (a) and nonchiral line (b) in the cavity.

The self-interaction magnetic field (for equilibrium magnetization along $\mathbf{y}$)

$$\tilde{H}^{(r)}_{\alpha\in\{x,z\}}(\mathbf{r},t) = \frac{\mu_0 V_s}{2\omega_m}\sum_\lambda \frac{1}{v(k_\lambda)} \times \left(|\mathscr{H}_{k_\lambda,\alpha}(\boldsymbol{\rho})|^2+|\mathscr{H}_{-k_\lambda,\alpha}(\boldsymbol{\rho})|^2\right)\frac{dM_\alpha(\mathbf{r},t)}{dt}, \quad (69)$$

is out-of-phase with the local magnetization and therefore acts like an additional and anisotropic Gilbert damping torque [21,22,24,25].

The linear response formulation [8,64] helps to understand the radiative damping: The precessing magnetization in a magnet radiates dipolar magnetic field that is out-of-phase with the magnetization. The self-interaction leads to a Gilbert dampinglike torque. This may be interpreted

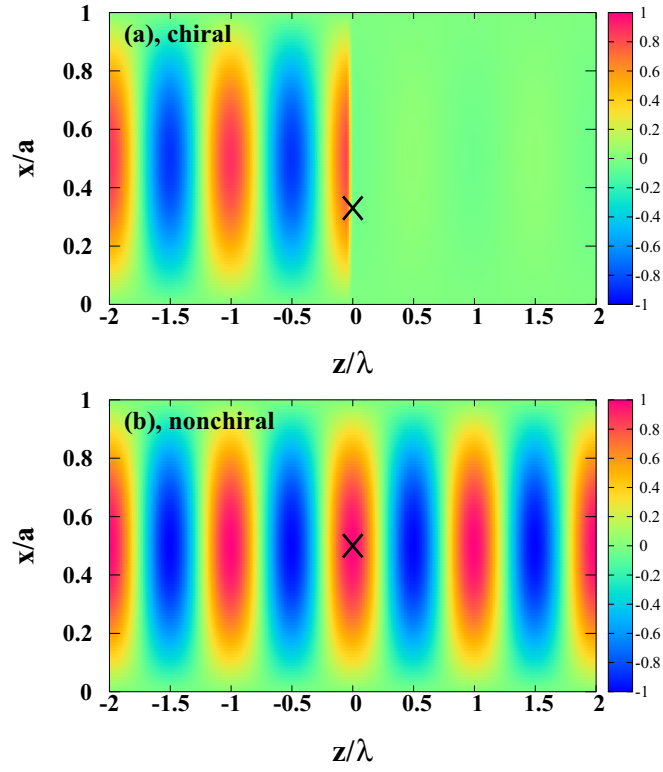

FIG. 4. Real-space magnetic field Eq. (66) (normalized to its maximum modulus and without near-field corrections) radiated by a magnetic sphere on a chiral [(a)] and nonchiral [(b)] line. The crosses indicate its position. The Kittel mode is tuned to $\omega_m = 2\sqrt{3}c\pi/a$ at which the photon wavelength $\lambda = 5.54$ cm.

in terms of pumping of energy and angular momentum into the microwave field. By substituting the linearized LLG equation [49],

$$\frac{dM_\alpha}{dt} = \varepsilon_{\alpha\beta\delta}M_\beta\left(-\tilde{\gamma}\mu_0 H_{\text{eff},\delta}+\tilde{\gamma}\mu_0\tilde{H}^{(r)}_\delta+\frac{\alpha_G}{M_s}\frac{dM_\delta}{dt}\right), \quad (70)$$

and the radiative damping is anisotropic:

$$\alpha^{(r)}_{\delta=\{x,z\}} = \frac{\mu_0^2 V_s}{2\omega_m}\sum_\lambda \frac{\tilde{\gamma}M_s}{v(k_\lambda)}\left(|\mathscr{H}_{k_\lambda,\delta}(\boldsymbol{\rho})|^2+|\mathscr{H}_{-k_\lambda,\delta}(\boldsymbol{\rho})|^2\right). \quad (71)$$

Linearizing Eq. (70) and substituting $M_\alpha \propto e^{-i\omega t}$ yields

$$\begin{aligned} i\omega M_x+(\tilde{\gamma}\mu_0 H_{\text{eff},y}-i\omega\alpha^{(r)}_z-i\omega\alpha_G)M_z = 0,\\ i\omega M_z-(\tilde{\gamma}\mu_0 H_{\text{eff},y}-i\omega\alpha^{(r)}_x-i\omega\alpha_G)M_x = 0, \end{aligned} \quad (72)$$

and the quadratic equation

$$\omega^2+i\omega\tilde{\gamma}\mu_0 H_{\text{eff},y}\left(\alpha^{(r)}_x+\alpha^{(r)}_z+2\alpha_G\right)-(\tilde{\gamma}\mu_0 H_{\text{eff},y})^2 = 0. \quad (73)$$

Therefore,

$$\alpha^{\text{eff}}_G(\omega) \approx \alpha_G+\left(\alpha^{(r)}_x+\alpha^{(r)}_z\right)/2 = \alpha_G+\alpha_r(\omega),$$

consistent with the equation of motion approach. The full damping tensor can in principle be reconstructed by computing the dependence of $\alpha^{(r)}_\delta$ on the magnetization direction.

V. MAGNON HYDROGEN MOLECULE

The interaction is nonlocal since the photons emitted by one magnet are reabsorbed by another magnet, which is a basically classical phenomenon (see Appendix C), even though we derived it by the Heisenberg equations of motion in Sec. II A and discussed in more detail for a rectangular waveguide in Sec. III. The classical electrodynamics in Appendix C becomes tedious for multiple magnets, so we focus in the following on the quantum description of two magnets, turning to the magnet chain in Sec. VI.

A. Collective mode

We consider the transmission of a single waveguide mode with input amplitude A_λ and frequency $\omega_{\rm in}$. In the following, we suppress the mode index λ, i.e., $A_\lambda = A$, $S_{12} \equiv S_{12}^{(\lambda\lambda)}$, $v \equiv v^{(\lambda)}(k_\lambda)$. $k \equiv k_\lambda$ is the wave vector of the incoming photons and $\mathscr{G} = (g_1, g_2)^T \equiv \mathscr{G}_{k_\lambda}^{(\lambda)}$ is the vector of couplings g_j of the jth magnet.

The two spheres are oriented along the waveguide with $\boldsymbol{\rho}_1 = \boldsymbol{\rho}_2$ and $d = z_2 > z_1 = 0$. The magnetic input field amplitude at the spheres differs by the phase kd. According to Sec. III,

$$\mathscr{G} = -ig_0(1\ e^{ikd})^T, \tag{74}$$

where g_0 is real. The frequency shift and radiative damping of the resonances in both magnets are the same and we absorb them into the complex frequencies ω_1, ω_2. The Hamiltonian matrix then reads

$$\tilde{H}_{\rm eff} = \tilde{\omega} + \Sigma = \begin{pmatrix} \omega_1 - i\alpha_G\omega_1 - i\frac{\Gamma_L+\Gamma_R}{2} & -i\Gamma_L e^{ikd} \\ -i\Gamma_R e^{ikd} & \omega_2 - i\alpha_G\omega_2 - i\frac{\Gamma_L+\Gamma_R}{2} \end{pmatrix}. \tag{75}$$

We assume $\omega_1 \approx \omega_2 \approx \omega_{\rm in}$, but allow them to vary in a window small enough that $\Gamma(\omega_1) \approx \Gamma(\omega_2) \approx \Gamma(\omega_{\rm in})$.

As discussed in Sec. II B, the eigenvectors of $\tilde{\omega} + \Sigma$, namely, $\{\psi_+, \psi_-\}$, with corresponding eigenvalues $\{\nu_+, \nu_-\}$ and eigenvectors of $(\tilde{\omega} + \Sigma)^\dagger$, namely, $\{\phi_+, \phi_-\}$ contain relevant information of the observables. Here

$$\begin{aligned} \nu_+ + \nu_- &= (\omega_2 + \omega_1)(1 - i\alpha_G) - i(\Gamma_L + \Gamma_R), \\ \nu_+ - \nu_- &= \sqrt{(\omega_2 - \omega_1)^2(1 - i\alpha_G)^2 - 4\Gamma_L\Gamma_R e^{2ikd}}, \end{aligned} \tag{76}$$

correspond to two resonant frequencies and linewidths. Assuming $1 - i\alpha_G \approx 1$,

$$\begin{aligned} \psi_\pm &\approx X_\pm \begin{pmatrix} \Delta \pm \sqrt{\Delta^2 - 4\Gamma_L\Gamma_R e^{2ikd}} \\ 2i\Gamma_R e^{ikd} \end{pmatrix}, \\ \phi_\pm &\approx Y_\pm \begin{pmatrix} 2i\Gamma_R e^{-ikd} \\ \Delta \mp \sqrt{\Delta^2 - 4\Gamma_L\Gamma_R e^{-2ikd}} \end{pmatrix}, \end{aligned} \tag{77}$$

with the detuning $\omega_2 - \omega_1 = \Delta$. The normalization factors

$$X_\pm Y_\pm^* = \frac{\pm i}{4\Gamma_R e^{ikd}\sqrt{\Delta^2 - 4\Gamma_L\Gamma_R e^{2ikd}}} \tag{78}$$

are chosen such that $\phi_\pm^\dagger \psi_\pm = 1$.

The absorption coefficient [Eq. (39)]

$$\begin{aligned} \mathscr{A}_\pm &= \phi_\pm^\dagger \mathscr{G} \\ &= -ig_0 Y_\pm^* e^{ikd}[\Delta - 2i\Gamma_R \mp \sqrt{\Delta^2 - 4\Gamma_L\Gamma_R e^{2ikd}}], \end{aligned} \tag{79}$$

and the excited magnetization can be written as

$$\langle \hat{\mathscr{M}} \rangle = \langle \hat{\alpha}_+(t) \rangle \psi_+ + \langle \hat{\alpha}_-(t) \rangle \psi_-, \tag{80}$$

with amplitudes [Eq. (40)]

$$\langle \hat{\alpha}_\pm(t) \rangle = Ae^{-i\omega_{\rm in}t} \frac{\mathscr{A}_\pm}{\omega_{\rm in} - \nu_\pm}. \tag{81}$$

B. Directional pumping of magnons

For zero detuning, the resonant input $\omega_{\rm in} = \omega_1 = \omega_2 = \omega_m$ drives the magnetization of each sphere into a coherent state $\langle \hat{m} \rangle$ with some thermal noise, see Sec. II C. The ratio of the coherent amplitudes,

$$\Lambda \triangleq \left| \frac{\langle \hat{m}_1 \rangle}{\langle \hat{m}_2 \rangle} \right| = \sqrt{\frac{\Gamma_L}{\Gamma_R}} \left| \frac{\langle \alpha_+ \rangle X_+ - \langle \alpha_- \rangle X_-}{\langle \alpha_+ \rangle X_+ + \langle \alpha_- \rangle X_-} \right|, \tag{82}$$

does not depend on time. With Eq. (81),

$$\Lambda = \left| \frac{2\alpha_G\omega_m + \Gamma_R + \Gamma_L(1 - 2e^{2ikd})}{2\alpha_G\omega_m + \Gamma_L - \Gamma_R} \right|. \tag{83}$$

Λ^2 is the ratio of the coherent magnon numbers (also refer to the results of the master equation below).

The imbalanced excitation $\Lambda \gg 1$ without chirality, i.e., when $\Gamma_L = \Gamma_R = \Gamma$: $\Lambda = |1 + 2\Gamma(1 - e^{2ikd})/(2\alpha_G\omega_m)|$ is caused by the direction of the feed and depends strongly on the parameters. When $\Gamma_R \to 0$ and $\Gamma_L \gg \alpha_G\omega_m$, we obtain the universal $\Lambda \approx \sqrt{5 - 4\cos(2kd)}$. When $kd = n\pi/2$ with n being odd integer, $\Lambda = 3$, and a ratio of the excited magnon numbers of $\Lambda^2 \approx 9$. When $\Gamma_L = \Gamma_R - 2\alpha_G\omega_m$, $|\langle \hat{m}_2 \rangle| = 0$ and Λ diverges, magnet 2 cannot be excited because the input and emitted photons from the other magnet interfere destructively. This limit can be realized by shifting the magnets in the waveguide and/or tuning the applied field. We summarize these features in Fig. 5 in terms of the magnon number imbalance Λ^2 in two magnets with fixed distance oriented along z and as a function of position in the waveguide cross section.

Magnons can also be excited locally by small local antennas with negligible crosstalk [1–4,9,10]. An imbalanced magnon excitation can be detected by the same antenna, as pioneered in the cavity experiment [20]. We can model local drives by adding source terms to the equation of motion Eq. (25),

$$\frac{d\langle \hat{\mathscr{M}} \rangle}{dt} = -i(\tilde{\omega} + \Sigma)\langle \hat{\mathscr{M}} \rangle + \begin{pmatrix} \langle \hat{P}_1(t) \rangle \\ \langle \hat{P}_2(t) \rangle \end{pmatrix}, \tag{84}$$

where $\hat{P}_i$ are the local magnetic field amplitudes and we ignored the dissipation caused by the local antennas for simplicity. When $\langle \hat{P}_i(t) \rangle = iPe^{-i\omega_{\rm in}t}$, where P is real,

$$\Lambda = \left| \frac{\Gamma_L + \Gamma_R + 2\alpha_G\omega_m - 2\Gamma_L e^{ikd}}{\Gamma_L + \Gamma_R + 2\alpha_G\omega_m - 2\Gamma_R e^{ikd}} \right|. \tag{85}$$

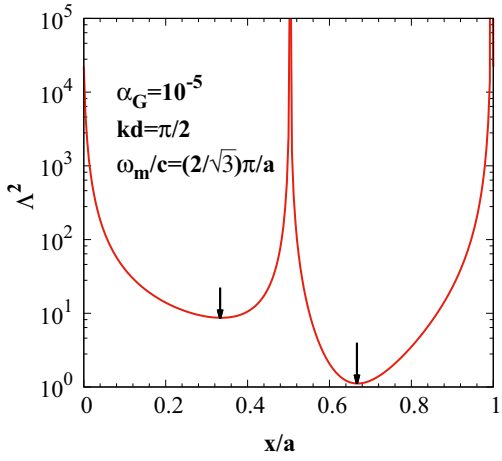

FIG. 5. Magnon number imbalance Λ^2 in a magnonic hyfrogen molecule in a waveguide, calculated as function of position by Eq. (83). The arrows indicate the positions of the chiral line. Note that Λ^2 is largest on the nonchiral lines at $x = 0, a/2$ and a. This is a geometrical effect that is suppressed for longer chains (see text).

In contrast to the waveguide drive discussed above, the excitation is balanced when $\Gamma_L = \Gamma_R$. $\Lambda \neq 1$ then requires chiral coupling, e.g., when $\Gamma_R = 0$, $\Lambda^2 \approx 5 - 4\cos(kd) \leqslant 9$. This imbalance is caused by the pumping of the first magnet by the second magnet without back action.

The coherent and dissipative components of the coupling emerge in the equation of motion from the commutator of the Hamiltonian with the magnon operator. Their different physical meanings can be understood best by the master equation [32,55,57,58]. To this end, we divide the non-Hermitian Hamiltonian into the Hermitian $\hat{H}_{\rm H}$ and non-Hermitian $\hat{H}_{\rm nH}$ parts as

$$\hat{H}_{\rm eff} = (\hat{H}_{\rm eff} + \hat{H}^\dagger_{\rm eff})/2 + (\hat{H}_{\rm eff} - \hat{H}^\dagger_{\rm eff})/2, \tag{86}$$

with the first and second terms representing the Hermitian and non-Hermitian parts, respectively. For the magnon hydrogen molecule,

$$\hat{H}_{\rm H} = \textstyle\sum_{i=1,2} \omega_i \hat{m}_i^\dagger \hat{m}_i + i\frac{\Sigma_{12}+\Sigma_{21}^*}{2}\hat{m}_1^\dagger \hat{m}_2 + i\frac{\Sigma_{21}+\Sigma_{12}^*}{2}\hat{m}_1 \hat{m}_2^\dagger, \tag{87}$$

$$\hat{H}_{\rm nH} = -i\textstyle\sum_{i=1,2} \frac{\delta\omega_m}{2}\hat{m}_i^\dagger \hat{m}_i + \frac{\Sigma_{12}-\Sigma_{21}^*}{2}\hat{m}_1^\dagger \hat{m}_2 + \frac{\Sigma_{21}-\Sigma_{12}^*}{2}\hat{m}_1^\dagger \hat{m}_2, \tag{88}$$

with $\delta\omega_m = \Gamma_R + \Gamma_L + 2\alpha_G\omega_m$, $\Sigma_{12} = -i\Gamma_L e^{ikd}$ and $\Sigma_{21} = -i\Gamma_R e^{ikd}$. The coherent and dissipative contribution cause different collective dampings [32,55,57,58]. The master equation for the density operator of magnon $\hat{\rho}$ [32,55,57,58],

$$\partial_t\hat{\rho} = i[\hat{\rho}, \hat{H}_{\rm H}] + \sum_i \frac{\delta\omega_m}{2}\hat{\mathscr{L}}_{ii}\hat{\rho} + i\frac{\Sigma_{12}-\Sigma_{21}^*}{2}\hat{\mathscr{L}}_{12}\hat{\rho} + i\frac{\Sigma_{21}-\Sigma_{12}^*}{2}\hat{\mathscr{L}}_{21}\hat{\rho}, \tag{89}$$

in which $\hat{\mathscr{L}}_{ij}\hat{\rho} = 2\hat{m}_j\hat{\rho}\hat{m}_i^\dagger - \hat{m}_i^\dagger\hat{m}_j\hat{\rho} - \hat{\rho}\hat{m}_i^\dagger\hat{m}_j$ is a relaxation operator (Lindblad super-operator), while $\delta\omega_m$ and $i(\Sigma_{12} - \Sigma_{21}^*)/2$ are the self- and collective decay rates, respectively. For perfect chiral coupling $\Sigma_{21} = 0$ and at resonance, the master equation in the rotating frame and $\hat{m}(t) = \tilde{m}e^{-i\omega_{\rm in}t}$ gives for the slowly varying envelopes $\tilde{m}_{1,2}$,

$$\frac{\partial}{\partial t}\begin{pmatrix}\langle\tilde{m}_1\rangle\\ \langle\tilde{m}_2\rangle\end{pmatrix} = \begin{pmatrix}-\delta\omega_m/2 & -i\Sigma_{12}\\ 0 & -\delta\omega_m/2\end{pmatrix}\begin{pmatrix}\langle\tilde{m}_1\rangle\\ \langle\tilde{m}_2\rangle\end{pmatrix} + (-iP - iP), \tag{90}$$

where the average $\langle\hat{O}(t)\rangle = \langle\hat{O}\hat{\rho}(t)\rangle$, and

$$\frac{\partial}{\partial t}\begin{pmatrix}\langle\tilde{m}_1^\dagger\tilde{m}_1\rangle\\ \langle\tilde{m}_2^\dagger\tilde{m}_2\rangle\\ \langle\tilde{m}_1^\dagger\tilde{m}_2\rangle\\ \langle\tilde{m}_1\tilde{m}_2^\dagger\rangle\end{pmatrix} = \begin{pmatrix}iP & -iP & 0 & 0\\ 0 & 0 & iP & -iP\\ 0 & -iP & iP & 0\\ -iP & 0 & 0 & iP\end{pmatrix}\begin{pmatrix}\langle\tilde{m}_1\rangle\\ \langle\tilde{m}_2\rangle\\ \langle\tilde{m}_1^\dagger\rangle\\ \langle\tilde{m}_2^\dagger\rangle\end{pmatrix} + \begin{pmatrix}-\delta\omega_m & 0 & -i\Sigma_{12} & i\Sigma_{12}^*\\ 0 & -\delta\omega_m & 0 & 0\\ 0 & \Sigma_{12}^* & -\delta\omega_m & 0\\ 0 & 0 & 0 & -\delta\omega_m\end{pmatrix}\begin{pmatrix}\langle\tilde{m}_1^\dagger\tilde{m}_1\rangle\\ \langle\tilde{m}_2^\dagger\tilde{m}_2\rangle\\ \langle\tilde{m}_1^\dagger\tilde{m}_2\rangle\\ \langle\tilde{m}_1\tilde{m}_2^\dagger\rangle\end{pmatrix}. \tag{91}$$

The coherent amplitude and associated magnon number (accumulation) obey different equations. P drives the coherent amplitude via Eq. (90), while the dissipative coupling in Eq. (91) causes collective damping of the magnon numbers. It can be easily shown that the master equation approach is equivalent to the input-output theory: Eqs. (90) and (91) recover the previous results for Λ and Λ^2 in Eq. (85).

VI. MAGNON CHAIN

The imbalance of the magnon distribution is enhanced when more magnets are added to the waveguide. Let us consider a chain of N identical magnets at equal distance $z_{j+1} - z_j = d$ $(0 < j < N)$ located on a line parallel to the wave guide. Such systems have already realized when $N = 7$ in a closed cavity [20]. We study the eigenvectors and eigenvalues of the non-Hermitian matrix

$$\tilde{H}_{\rm eff} = \begin{pmatrix}\omega_m - i\alpha_G\omega_m - i\frac{\Gamma_R+\Gamma_L}{2} & -i\Gamma_L e^{ikd} & -i\Gamma_L e^{2ikd} & \dots & -i\Gamma_L e^{(N-1)ikd}\\ -i\Gamma_R e^{ikd} & \omega_m - i\alpha_G\omega_m - i\frac{\Gamma_R+\Gamma_L}{2} & -i\Gamma_L e^{ikd} & \dots & -i\Gamma_L e^{(N-2)ikd}\\ -i\Gamma_R e^{2ikd} & -i\Gamma_R e^{ikd} & \omega_m - i\alpha_G\omega_m - i\frac{\Gamma_R+\Gamma_L}{2} & \dots & -i\Gamma_L e^{(N-3)kd}\\ \vdots & \vdots & \vdots & \ddots & \vdots\\ -i\Gamma_R e^{i(N-1)kd} & -i\Gamma_R e^{i(N-2)kd} & -i\Gamma_R e^{i(N-3)kd} & \dots & \omega_m - i\alpha_G\omega_m - i\frac{\Gamma_R+\Gamma_L}{2}\end{pmatrix}, \tag{92}$$

where we dropped the TE_{10} mode index λ and

$$k = \sqrt{\frac{\omega_m^2}{c^2} - \left(\frac{\pi}{a}\right)^2}. \tag{93}$$

The photons emitted by magnet j to the right are in our perturbative and adiabatic approach seen equivalently and instantaneously by all magnets on the right but with a phase factor $e^{ik|z_j - z_l|}$, and analogously for the magnets to the left.

The photon-mediated interaction generates a band structure with generalized Bloch states labeled $\zeta \in \{1, \ldots, N\}$ with right eigenvectors $\{\psi_\zeta\}$ and corresponding eigenvalues $\{\nu_\zeta\}$:

$$(\nu_\zeta - \tilde{H}_{\rm eff})\psi_\zeta = 0. \tag{94}$$

The real part of ν_ζ is the resonance frequency of the ζ mode and the imaginary part its lifetime. The eigenvectors of $\tilde{H}_{\rm eff}^\dagger$, ϕ_ζ with eigenvalue ν_ζ^* are related to ψ_ζ by a parity-time reversal operation when the spectrum is not degenerate, which is the case for the simple chain considered here. Let $\mathscr{T}$ be the complex conjugation and

$$\mathscr{P} = \begin{pmatrix} 0 & 0 & \ldots & 0 & 1 \\ 0 & 0 & \ldots & 1 & 0 \\ \vdots & \vdots & \ddots & \vdots & \vdots \\ 0 & 1 & \ldots & 0 & 0 \\ 1 & 0 & \ldots & 0 & 0 \end{pmatrix} \tag{95}$$

exchanges the magnets $1 \leftrightarrow N$, $2 \leftrightarrow N-1$ and so on, akin to the inversion operation. However, $\mathscr{P}$ does not act on the waveguide and is therefore not a parity operator of the whole system. Clearly, $\mathscr{P}^2 = \mathscr{T}^2 = 1$. $\mathscr{P}$ interchanges $\Gamma_{L\leftrightarrow R}$ in Eq. (92), which is equivalent to the transpose operation, i.e., $\tilde{H}_{\rm eff}^T = \mathscr{P}\tilde{H}_{\rm eff}\mathscr{P}$, while $\tilde{H}_{\rm eff}^\dagger = \mathscr{P}\mathscr{T}\tilde{H}_{\rm eff}\mathscr{T}\mathscr{P}$ and

$$\tilde{H}_{\rm eff}^\dagger \mathscr{P}\mathscr{T}\psi_\zeta = \nu_\zeta^* \mathscr{P}\mathscr{T}\psi_\zeta, \tag{96}$$

implying that

$$\phi_\zeta = \mathscr{P}\mathscr{T}\psi_\zeta. \tag{97}$$

We chose a normalization

$$\psi_\zeta^T \mathscr{P}\psi_\zeta = 1, \tag{98}$$

such that $\phi_\zeta^\dagger \psi_\zeta = 1$. Thus, we can describe the dynamics in terms of only the right eigenvectors ψ_ζ.

The magnets interact with the photons (again suppressing indices) by the phase vector

$$\mathscr{G} = -i\sqrt{\Gamma_R v}(1, e^{ikd}, \ldots, e^{i(N-1)kd})^T. \tag{99}$$

The emission amplitude $\mathscr{E}_\zeta = \mathscr{G}^\dagger\psi_\zeta = i\sqrt{\Gamma_R v}\tilde{\psi}_\zeta(k)$, where we defined the discrete Fourier transform

$$\tilde{\psi}_\zeta(k) = (1, e^{-ikd}, \ldots, e^{-i(N-1)kd})^T\psi_\zeta. \tag{100}$$

The absorption amplitude $\mathscr{A}_\zeta = \phi_\zeta^\dagger\mathscr{G}$ is related to the emission by

$$\mathscr{A}_\zeta = e^{i(N-1)kd}\mathscr{E}_\zeta. \tag{101}$$

The global transmission [cf. Eq. (44)]

$$S_{12}(\omega_{\rm in}) = 1 - i\Gamma_R e^{i(N-1)kd}\sum_\zeta \frac{\tilde{\psi}_\zeta^2(k)}{\omega_{\rm in} - \nu_\zeta}, \tag{102}$$

is governed by the right eigenvectors. The total coherent magnetization of the array

$$\langle\hat{\mathscr{M}}(t)\rangle = A\sqrt{\Gamma_R v}e^{-i\omega_{\rm in}t}e^{i(N-1)kd}\sum_\zeta \frac{\tilde{\psi}_\zeta(k)}{\omega_{\rm in} - \nu_\zeta}\psi_\zeta \tag{103}$$

is proportional to the amplitude of the incoming photons A (introduced in Sec. II C).

Magnons can be flexibly excited and detected by local antennas that interact only with one magnet [20]. With local input at frequency $\omega_{\rm in}$, $\langle\hat{\mathscr{T}}_l(t)\rangle = ie^{-i\omega_{\rm in}t}(P_1, P_2, \cdots, P_N)^T$,

$$\langle\hat{\mathscr{M}}(t)\rangle = -i\sum_\zeta \frac{(\mathscr{P}\psi_\zeta)^T\langle\hat{\mathscr{T}}_l(t)\rangle}{\omega_{\rm in} - \tilde{\omega}_m - \gamma_\zeta}\psi_\zeta. \tag{104}$$

Note that $(\mathscr{P}\psi_\zeta)^T = (\psi_{\zeta,N}, \psi_{\zeta,N-1}, \cdots, \psi_1)$. When an edge state ζ_* exists, say on the right with large $\psi_{\zeta,N}$, the antenna array with controlled phase difference ϕ, i.e., $\langle\hat{\mathscr{T}}_l(t)\rangle = \exp[-i{\rm Re}(\gamma_{\zeta_*})t]iP(1, e^{i\phi}, \cdots, e^{i(N-1)\phi})^T$, can excite a large magnetization at the right edge, where it can be detected by the same local antenna as pointed out in the accompanying letter [46].

We see that the excitation of magnetization is determined by the eigenvectors ψ_ζ and their eigenvalues ν_ζ, which are studied numerically and analytically below, with special attention for superradiant and subradiant modes, i.e., those with the largest and smallest radiation rates, respectively.

A. Numerical results

We present and analyze numerical results for the collective modes of the dissipatively coupled magnon chain. As before, $a = 1.6\,{\rm cm}$, $b = 0.6\,{\rm cm}$, $r_s = 0.6\,{\rm mm}$, and $\alpha_G = 5 \times 10^{-5}$ [23]. Typically, $\omega_m/c = \sqrt{3}\pi/a$ corresponding to the photon momentum $k = \sqrt{2}\pi/a$, so only the lowest TE_{10} mode contributes. The magnetic chain is parallel to the waveguide and shifted from the chiral line to modulate the chirality $\Gamma_R/\Gamma_L = 1, 0.5, 0.25$, where $\Gamma_L/(2\pi) \in (0, 20)\,{\rm MHz}$. We choose $N = 80$ magnetic spheres and $kd = 3\pi/5$. So $d = a/(5\sqrt{3}) \approx 0.6\,{\rm cm}$ and the total length of the magnon chain is $Nd \approx 48\,{\rm cm}$. This is longer than our choice in the accompanying letter [46] and experimentally impractical, but the results are not qualitatively different and emphasize our message.

Figure 6 is a plot of the imaginary (Γ_ζ) and real (E_ζ) parts of $\nu_\zeta - \omega_m$ as a function of mode number ζ, scaled by the local dissipation rate $\Gamma_a = \alpha_G\omega_m + (\Gamma_L + \Gamma_R)/2$. The mode numbers $\zeta = \{1, 2, ..., N\}$ are ordered by magnitudes of Γ_ζ.

When $\Gamma_R = \Gamma_L$ (nonchiral case) and $\zeta \approx 80$ ($\zeta \lesssim 10$), the decay rates are larger (smaller) than the local Γ_a, indicating superradiance (subradiance). The decay rates of the most superradiant states $\sim\Gamma_a N/4$ can simply be enhanced by increasing the number of magnets. The decay of the most subradiant states $\sim\Gamma_a\zeta^2/N^3$ [39–43] are found at the lower band edge. The value of the magnon energy shifts E_ζ in the inset of Fig. 6 are enhanced to a peak around the boundary between sub- and superradiance ($\Gamma_\zeta \approx \Gamma_a$). E_ζ and Γ_ζ don't have a simple functional relationship, which is reflected by the oscillations (peaks) that look erratic for small mode numbers. The energy shift of the most subradiant states is very small but it can be as large as $\sim 10\Gamma_a$ for the superradiant ones, roughly proportional to the number of magnets. The largest

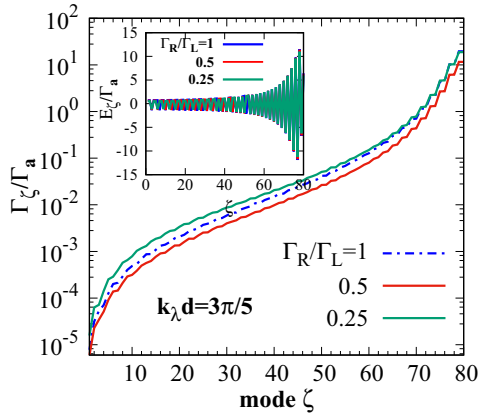

FIG. 6. Imaginary (Γ_ζ) and real (inset, E_ζ) parts of the eigenvalues ($\nu_\zeta - \omega_m$) of the non-Hermitian Hamiltonian [Eq. (92)], scaled by the individual damping rate Γ_a . $k_\lambda d = 3\pi/5$ and $N = 80$. $\Gamma_R/\Gamma_L = 1$, 0.5 and 0.25, respectively. E_ζ oscillates as a function of ζ and Γ_ζ in a nonsystematic manner.

energy shift $2\pi \times 100\,\mathrm{MHz}$ is still small compared to ω_m, which justifies the on-shell approximation for Γ_L and Γ_R. E_ζ oscillates with ζ between positive and negative values. A chiral coupling with $\Gamma_R/\Gamma_L = 0.5$ and 0.25 does not strongly change the above features, such the decay rates of the most subradiant states $\sim\Gamma_a\zeta^2/N^3$.

The intensity distributions $|\psi_{\zeta,j}|^2$ of modes $\zeta = 1, 2, 80$ over the chain $j = \{1, 2, \cdots, N\}$ are shown in Fig. 7. When $\Gamma_R = \Gamma_L$ for the nonchiral case, the most superradiant state is enhanced at both edges of the magnon chain (the red solid curve). The most subradiant states are standing waves $\sim|\sin(\zeta\pi j/N)|$ delocalized over the whole chain, but have small amplitudes at the edges (see the inset of Fig. 7).

Partially chiral coupling does not affect the amplitude distributions of the most subradiant states. The symmetric distribution of the most superradiant states relative to the center of the chain $\Gamma_R = \Gamma_L$ becomes increasingly skewed, i.e., the dynamics is enhanced at one edge only. Particularly, when $\Gamma_R < \Gamma_L$ ($\Gamma_R > \Gamma_L$), the edge state is localized at the

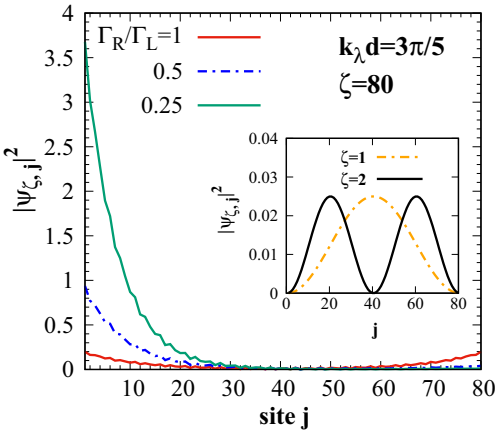

FIG. 7. Intensity distributions of magnons $|\psi_{\zeta,j}|^2$ in magnetic spheres labeled by j for the most superadiant and subradiant (inset) states for chiralities $\Gamma_R/\Gamma_L = 1$, 0.5, and 0.25, respectively.

left (right) side. When the radiation to the left is stronger than to the right, the magnets on the left side experience more radiation. On the other hand, the magnets in the middle of the chain are part of a standing wave with destructive interference in the average. A larger chirality Γ_R/Γ_L consequently mainly affects the edge states.

B. Analytical analysis

The rich features of the collective motion in the most-sub- and superradiant states can be accessed analytically in some special limits [40]. To this end, we search for linear combinations of the magnon operators $\hat{\alpha}$ that satisfy $d\hat{\alpha}/dt = -i\nu\hat{\alpha} + (\text{noise})$ as discussed in Sec. II B.

We can rewrite the equation of motion for the magnetization, Eq. (25), as

$$\frac{d}{dt}(\hat{m}_1, \hat{m}_2, \cdots, \hat{m}_\delta)^T = -i\tilde{H}_{\text{eff}}(\hat{m}_1, \hat{m}_2, \cdots, \hat{m}_\delta)^T. \quad (105)$$

Inserting Eq. (92) for the magnon chain leads to

$$-\left(\frac{d\hat{m}_\delta}{dt}\right)_c = \frac{\Gamma_R + \Gamma_L}{2}\hat{m}_\delta + \Gamma_R\sum_{j<\delta} e^{ikd(\delta-j)}\hat{m}_j + \Gamma_L\sum_{j>\delta} e^{ikd(j-\delta)}\hat{m}_j. \quad (106)$$

where we dropped the noise term and the self-interaction $\propto i\omega\hat{m}_\delta$ that only contributes a constant, but does not affect the eigenmodes. Inserting a trial Bloch state with complex momentum κ,

$$\hat{m}_\delta \to \hat{\Psi}_\kappa = \frac{1}{\sqrt{N}}\sum_{j=1}^{N} e^{i\kappa z_j}\hat{m}_j \quad (107)$$

into Eq. (106) leads to

$$\left(\frac{d\hat{\Psi}_\kappa}{dt}\right)_c = -i\omega_\kappa\hat{\Psi}_\kappa - \Gamma_L g_\kappa\hat{\Psi}_k + \Gamma_R h_\kappa\hat{\Psi}_{-k}, \quad (108)$$

with complex dispersion relation

$$\omega_\kappa = -i\frac{\Gamma_R}{2}\frac{1+e^{i(\kappa+k)d}}{1-e^{i(\kappa+k)d}} + i\frac{\Gamma_L}{2}\frac{1+e^{i(\kappa-k)d}}{1-e^{i(\kappa-k)d}}, \quad (109)$$

and "leakage" parameters

$$g_\kappa = \frac{1}{1-e^{i(\kappa-k)d}}, \quad h_\kappa = \frac{e^{i(\kappa+k)Nd}}{1-e^{i(\kappa+k)d}}. \quad (110)$$

Equation (108) is a closed equation for the unknown κ. Only when the terms g_κ, h_κ in Eq. (108) vanish is $\hat{\Psi}_\kappa$ a proper solution. The leakage and reflection at the edges mixes $\hat{\Psi}_\kappa$ with the plane waves $\hat{\Psi}_k$ and $\hat{\Psi}_{-k}$, which renders the problem nontrivial.

In general, the field operator $\hat{\alpha}$ should be a superposition of frequency-degenerate Bloch waves. For the simple chain, two states with κ and κ' should suffice, provided

$$\omega_\kappa = \omega_{\kappa'}, \quad (111)$$

which leads to $(\Gamma_R - \Gamma_L + 2\omega_\kappa)/(\Gamma_R + \Gamma_L + 2\omega_\kappa) = -e^{i(\kappa'+\kappa)d}$. Trying $\hat{\alpha} = g_{\kappa'}\hat{\Psi}_\kappa - g_\kappa\hat{\Psi}_{\kappa'}$ gives

$$\left(\frac{d\hat{\alpha}}{dt}\right)_c = -i\omega_\kappa\hat{\alpha} + \Gamma_R(g_{\kappa'}h_\kappa - g_\kappa h_{\kappa'})\hat{\Psi}_{-k}, \quad (112)$$

which is the desired equation when

$$g_\kappa h_{\kappa'} = g_{\kappa'} h_\kappa. \tag{113}$$

Equation (113) is an Nth-order polynomial equation in $e^{i\kappa_\zeta d}$ with N roots. Since we have N magnets and modes in the noninteracting limits, its solutions cover all eigenvalues of the interacting system. Equations (111) and (113) suffice to determine the complex unknown variables κ and κ'. The wave function and energies of collective mode can then be expanded as $\hat{\alpha}_\zeta = \sum_j \phi^*_{\zeta,j}\hat{m}_j$ and with

$$\hat{\alpha} = \frac{1}{\sqrt{N}}\sum_{j=1}^{N}(g_{\kappa'}e^{ikz_j} - g_\kappa e^{ik'z_j})\hat{m}_j, \tag{114}$$

we obtain

$$\phi^*_j = g_{\kappa'}e^{ikz_j} - g_\kappa e^{ik'z_j}. \tag{115}$$

Using the relation between the left and right eigenvectors [Eq. (97)], $\phi^* = P\psi$,

$$\psi_j \propto g_{\kappa'}e^{i\kappa z_{N-j}} - g_\kappa e^{ik'z_{N-j}}, \tag{116}$$

$$\nu = \tilde{\omega}_m + \omega_\kappa, \tag{117}$$

with $z_j = (j-1)d$ and the normalization of ψ_ζ is given by Eq. (98). For $\Gamma_L = \Gamma_R$, we find $\kappa' = -\kappa$ [40].

The imaginary part of $\omega_\kappa = \omega_{\kappa'}$ corresponds to the radiative damping of the mode ζ. The superradiant modes with $\mathrm{Im}\omega_\kappa \gg \Gamma_R, \Gamma_L$ are near $\kappa \approx \pm k$, i.e., complex momenta $\kappa = k_0 + \eta$ and $\kappa' = -k_0 + \eta'$ with small complex numbers η and η', which have to be calculated numerically. The imaginary part of η and η' are reciprocal skin depths of the edge states addressed in Sec. VI A.

Near the minima of ω_κ, around say $\kappa = \kappa_*$, we expect subradiant modes. Minimizing Eq. (109) leads to

$$\kappa_* d = \arcsin\frac{\Gamma_R - \Gamma_L}{\sqrt{\Gamma_R^2 + \Gamma_L^2 - 2\Gamma_R\Gamma_L\cos(2kd)}} - \arctan\frac{\Gamma_R - \Gamma_L}{(\Gamma_R + \Gamma_L)\tan(kd)}. \tag{118}$$

The arcsin is a two-valued function and hence we search for two extremal points in the first Brillouin zone $[-\pi/d, \pi/d]$. κ_* and the corresponding κ'_* do not yet satisfy the eigenvalue Eq. (113). Trying $\kappa = \kappa_* + \delta$ and $\kappa' = \kappa_* - \delta$ leads to

$$e^{2i\delta Nd} = \frac{\cos(\kappa_* d) - \cos[(k+\delta)d]}{\cos(\kappa_* d) - \cos[(k-\delta)d]}. \tag{119}$$

For $|\delta d| \ll 1$,

$$\delta \approx \frac{\xi\pi}{Nd}\left[1 - \frac{i}{N}\frac{\sin(kd)}{\cos(\kappa_* d) - \cos(kd)}\right], \tag{120}$$

where $\xi = \{1, 2, \cdots\}$, leading to eigenfunctions

$$\psi_{\xi,j} \approx -2i\frac{e^{i\kappa_* z_{N-j}}}{1 - e^{i(\kappa_* - k)d}}\sin(\delta_\xi z_{N-j}),$$
$$\omega_\xi = \omega_{\kappa_*} + \frac{\sin(kd)}{\cos(\kappa_* d) - \cos(kd)}\frac{\Gamma_R(\delta_\xi d)^2/2}{1 - \cos[(k+\kappa_*)d]}, \tag{121}$$

that are symmetric even for chiral coupling, because subradiant modes do not efficiently couple to the waveguide. These results also explain the standing-wave feature and scaling law of the radiative lifetime of these states.

VII. DISCUSSION AND CONCLUSION

In conclusion, we find and report the consequences of chiral and dissipative coupling of small magnets to guided microwaves. We predict a rich variety of physical phenomena, such as directional photon emission and magnon imbalanced pumping and super(sub)radiance of collective magnon modes. Polarization-momentum locking of the electromagnetic field inside a rectangular waveguide and conservation of angular momentum are the physical mechanisms behind chiral magnon-photons interaction. Chirality can be tuned via the positions of the magnetic spheres inside the waveguide and applied static magnetic fields. We develop the theory starting with a single magnet and demonstrate strong radiative damping. Loading the waveguide with two or more magnets causes nonreciprocal tunable coupling between different magnetic spheres. We predict chirality-dependent large magnon amplitudes at the edges of long chains with superradiance. We also reveal subradiant eigenstates, which are standing waves with small amplitude at the edges, that depend only weakly on chirality and therefore scale as different systems without chirality [39–44].

The magnetic chain in a waveguide is also a platform to study non-Hermitian physics [68–72]. The rich magnon-photon dynamics suggests several lines of future research. Tunable waveguides allow manipulation of the local density of photon states and linewidth for each collective mode [23], while arrangements of the magnetic spheres into rings, lattices, or random geometry promise a "magnon chemistry." Some non-Hermitian Hamiltonians may result in topological phases, a hot topic in condensed-matter physics [45,73–76]. The non-Bloch-wave behavior of eigenstates of a chiral magnon-photon system can cause a non-Hermitian skin effect and a non-Bloch bulk-boundary correspondence. The nonlinear dynamics of a chiral versus nonchiral magnon-photon system can be accessed by the photon statistics of the waveguide to specify the entanglement of sub- and superradiant states [43].

ACKNOWLEDGMENTS

This work is financially supported by the Nederlandse Organisatie voor Wetenschappelijk Onderzoek (NWO) as well as JSPS KAKENHI Grant No. 26103006. We would like to thank Yu-Xiang Zhang and Bi-Mu Yao for helpful discussions.

APPENDIX A: DISSIPATIVE COUPLING

Here we derive the radiative damping and dissipative coupling between identical magnets in a rectangular waveguide by photons in both TM and TE modes by explicitly calculating Eq. (30). For simplicity, we drop the explicit dependence on λ and k, i.e., $\Omega \equiv \Omega_k^\lambda$ and $g_j \equiv g_j^\lambda(k)$.

The magnetic field of the TM modes [26]

$$\begin{aligned}\mathscr{H}_x &= \sqrt{\tfrac{2\hbar\Omega}{\mu_0 ab}}\tfrac{\gamma_y}{\gamma}\sin(\gamma_x x)\cos(\gamma_y y),\\ \mathscr{H}_y &= -\sqrt{\tfrac{2\hbar\Omega}{\mu_0 ab}}\tfrac{\gamma_x}{\gamma}\cos(\gamma_x x)\sin(\gamma_y y),\end{aligned} \tag{A1}$$

with both $n_x, n_y > 0$, and of the TE modes

$$\begin{aligned}\mathscr{H}_z &= -i\sqrt{\tfrac{\eta\hbar\Omega}{\mu_0 ab}}\tfrac{c\gamma}{\Omega}\tfrac{|k|}{k}\cos(\gamma_x x)\cos(\gamma_y y),\\ \mathscr{H}_x &= -\sqrt{\tfrac{\eta\hbar\Omega}{\mu_0 ab}}\tfrac{c|k|}{\Omega}\tfrac{\gamma_x}{\gamma}\sin(\gamma_x x)\cos(\gamma_y y),\\ \mathscr{H}_y &= -\sqrt{\tfrac{\eta\hbar\Omega}{\mu_0 ab}}\tfrac{c|k|}{\Omega}\tfrac{\gamma_y}{\gamma}\cos(\gamma_x x)\sin(\gamma_y y),\end{aligned} \tag{A2}$$

in which $\eta = 2 - \delta_{n_x,0} - \delta_{n_y,0}$ and at least one $n_x, n_y > 0$. According to Eq. (14),

$$g_j^{\mathrm{TM}} = i\sqrt{\frac{\tilde{\gamma}\mu_0 M_s V_s \Omega}{ab}}\frac{\gamma_y}{\gamma}e^{ikz_j}\sin(\gamma_x x_j)\cos(\gamma_y y_j) \tag{A3}$$

and

$$\begin{aligned}g_j^{\mathrm{TE}} = i\sqrt{\frac{\eta\tilde{\gamma}\mu_0 M_s V_s \Omega}{ab}}\frac{c|k|}{\Omega}\frac{\gamma_x}{\gamma}e^{ikz_j}\cos(\gamma_y y_j)\\ \times\left[-\sin(\gamma_x x_j) + \frac{\gamma^2}{k\gamma_x}\cos(\gamma_x x_j)\right].\end{aligned} \tag{A4}$$

At large $|k|$, these couplings increase proportionally to $\sqrt{|k|}$ because the magnetic field scales with the square-root of the photon energy. The magnon-magnon coupling in Eq. (30) then becomes

$$\begin{aligned}\Sigma_{jl} = \frac{\tilde{\gamma}\mu_0 M_s V_s}{ab}\sum_{n_x,n_y}\sin(\gamma_x x_j)\cos(\gamma_y y_j)\\ \times\sin(\gamma_y x_l)\cos(\gamma_y y_l)\left(\frac{\gamma_y^2}{\gamma^2}\mathscr{I}_{\mathrm{TM}} + \frac{\gamma_x^2}{\gamma^2}\mathscr{I}_{\mathrm{TE}}\right),\end{aligned} \tag{A5}$$

where the $\mathscr{I}_\sigma$ summarize the TM and TE contributions. Here

$$\mathscr{I}_{\mathrm{TM}} = \int\frac{\Omega e^{ik(z_j-z_l)}}{\omega_l - \Omega + i0^+}\frac{dk}{2\pi}. \tag{A6}$$

The ultraviolet divergence for $z_j = z_l$ can be removed by introducing a cutoff momentum k_c that parametrizes dissipation in the metal boundaries at high frequencies:

$$\mathscr{I}_{\mathrm{TM}}|_{j=l} = \int_{-\infty}^{\infty}\frac{dk}{2\pi}\frac{\omega_l}{\omega_l - \Omega + i0^+} - 2k_c\delta_{jl}. \tag{A7}$$

Using the Cauchy's relation $1/(x+i0^+) = \mathscr{P}(1/x) - i\pi\delta(x)$, where $\mathscr{P}$ is the principle value,

$$\mathscr{I}_{\mathrm{TM}}|_{j=l} = -i\omega_l^2/(c^2 k_l) - 2k_c, \tag{A8}$$

where $k_l = \sqrt{\omega_l^2/c^2 - \gamma^2}$ with $\omega_l \geqslant \gamma c$. The divergence of the imaginary part at the band edge $\omega_l \approx c\gamma$ is a harmless van Hove singularity.

When $z_j > z_l$ and $\gamma|z_j - z_l| > 1$, the photon mode with negative wave number is evanescent and cannot affect another magnet that is not in immediate proximity. The integral then simplifies to

$$\mathscr{I}_{\mathrm{TM}}|_{z_j>z_l} = \int_{-\infty}^{\infty}\frac{dk}{2\pi}\frac{\Omega e^{ik(z_j-z_l)}}{\omega_l - \Omega + i0^+} \approx \frac{i\omega_l^2 e^{ik_l(z_j-z_l)}}{c^2 k_l},$$

consistent with Ref. [26], Sec. IV B, and our numerical calculations. The restriction $2\pi(z_j - z_l) \gtrsim \min\{a, b\}$ (or $k_l(z_j - z_l) > 1$) requires that for our system $z_j - z_l \gtrsim 0.2\,\mathrm{cm}$ for $\min\{a, b\} \sim 1\,\mathrm{cm}$, which we assume to be the case in the following. For $z_j < z_l$, a similar result holds with $z_j - z_l \to z_l - z_j$.

For TE modes,

$$\mathscr{I}_{\mathrm{TE}} = \int\frac{dk}{2\pi}\frac{c^2 e^{ik(z_j-z_l)}}{\Omega(\omega_l - \Omega + i0^+)}\left[-k + \frac{\gamma^2}{\gamma_x}\cot(\gamma_x x_j)\right]^2. \tag{A9}$$

We obtain

$$\mathscr{I}_{\mathrm{TE}}|_{j=l} = -i\frac{1}{k_l}\left[k_l^2 + \frac{\gamma^4}{\gamma_x^2}\cot^2(\gamma_x x_j)\right] - 2k_c. \tag{A10}$$

When $\gamma|z_j - z_l| > 1$,

$$\mathscr{I}_{\mathrm{TE}}|_{z_j-z_l} = -i\frac{e^{ik_l|z_j-z_l|}}{k_l}\left[-k_l + \frac{\gamma^2}{\gamma_x}\cot(\gamma_x x_j)\right]^2. \tag{A11}$$

APPENDIX B: FREE-SPACE RADIATION DAMPING

Here we drive the radiation damping of the Kittel mode of a single magnet in free space addressed in Sec. II. The magnetic field can be expanded:

$$\mathbf{H}(\mathbf{r}) = \sum_\sigma\int\frac{d^3k}{(\sqrt{2\pi})^3}\sqrt{\frac{\hbar\Omega_k}{2\mu_0}}\mathbf{e}_{\mathbf{k}}^\sigma(e^{i\mathbf{k}.\mathbf{r}}\hat{p}_{\mathbf{k}} + e^{-i\mathbf{k}.\mathbf{r}}\hat{p}_{\mathbf{k}}^\dagger). \tag{B1}$$

The frequency $\Omega_k = ck$ and the two polarization vectors are

$$\mathbf{e}_{\mathbf{k}}^1 = \frac{(k_z, 0, -k_x)}{\sqrt{k_x^2 + k_z^2}},\quad \mathbf{e}_{\mathbf{k}}^2 = \frac{k_y\mathbf{k} - k^2\mathbf{y}}{k\sqrt{k_x^2 + k_z^2}}. \tag{B2}$$

The coupling with a magnet with equilibrium magnetization along $\mathbf{y}$:

$$g_{\mathbf{k}}^\sigma = \sqrt{\frac{\mu_0\Omega_k}{2}\frac{\gamma M_s V_s}{2}}\left(ie_{\mathbf{k},x}^\sigma - ie_{\mathbf{k},z}^\sigma\right). \tag{B3}$$

The broadening of the ferromagnetic resonance is given by Fermi's golden rule [analogous to Eq. (58)],

$$\Delta\omega = \sum_\sigma\int\frac{d^3k}{(2\pi)^2}\delta(\omega_m - \Omega_k)\left|g_{\mathbf{k}}^\sigma\right|^2, \tag{B4}$$

where ω_m is the magnon frequency. $|g_{\mathbf{k}}^\sigma|^2$ can be simplified by the relations

$$\left|ie_{\mathbf{k},x}^1 - e_{\mathbf{k},z}^1\right|^2 = 1,\quad \left|ie_{\mathbf{k},x}^2 - e_{\mathbf{k},z}^2\right|^2 = \frac{k_y^2}{k^2}. \tag{B5}$$

In polar coordinates, with $k_y = k\cos\theta$:

$$\frac{\Delta\omega}{\omega_m} = \frac{\gamma\mu_0 M_s V_s\omega_m^2}{4c^3}\int\sin\theta d\theta d\phi\left(1 + \cos^2\theta\right), \tag{B6}$$

$$= \frac{\gamma\mu_0 M_s V_s\omega_m^2}{3\pi c^3}. \tag{B7}$$

This result agrees with theory and experiments on mm-sized spheres [21,22].

APPENDIX C: CLASSICAL DESCRIPTION OF MAGNET-MAGNET COUPLING

Here we formulate the nonlocal dissipative coupling of the magnetization dynamics in a waveguide by the classical LLG equation. We can incorporate the dynamic magnetic fields $\tilde{\mathbf{H}}^r_{2\to1}$ and $\tilde{\mathbf{H}}^r_{1\to2}$ between two magnetic spheres as [8]

$$\frac{dM_{1,\alpha}}{dt} = -\gamma\mu_0\varepsilon_{\alpha\beta\delta}M_{1,\beta}H^{\rm eff}_{1,\delta} + \gamma\mu_0\varepsilon_{\alpha\beta\delta}M_{1,\beta}\tilde{H}^r_{2\to1,\delta} + \frac{\alpha_G+\alpha^r_{1,\delta}}{M_{1,s}}\varepsilon_{\alpha\beta\delta}M_{1,\beta}\frac{dM_{1,\delta}}{dt}, \tag{C1}$$

$$\frac{dM_{2,\alpha}}{dt} = -\gamma\mu_0\varepsilon_{\alpha\beta\delta}M_{2,\beta}H^{\rm eff}_{2,\delta} + \gamma\mu_0\varepsilon_{\alpha\beta\delta}M_{2,\beta}\tilde{H}^r_{1\to2,\delta} + \frac{\alpha_G+\alpha^r_{2,\delta}}{M_{2,s}}\varepsilon_{\alpha\beta\delta}M_{2,\beta}\frac{dM_{2,\delta}}{dt}. \tag{C2}$$

The magnetic fields from Eq. (68) read for $z_1 > z_2$,

$$\tilde{H}^r_{2\to1,\delta}(\mathbf{r}_1,t) = -i\frac{\mu_0V_s}{v(k_\omega)}\mathscr{H}_{k_\omega,\delta}(\boldsymbol{\rho}_1)\mathscr{H}^*_{k_\omega,\eta}(\boldsymbol{\rho}_2)M_{2,\eta} \times e^{ik_\omega(z_1-z_2)}, \tag{C3}$$

$$\tilde{H}^r_{1\to2,\delta}(\mathbf{r}_2,t) = -i\frac{\mu_0V_s}{v(k_\omega)}\mathscr{H}_{-k_\omega,\delta}(\boldsymbol{\rho}_2)\mathscr{H}^*_{-k_\omega,\eta}(\boldsymbol{\rho}_1)M_{1,\eta} \times e^{ik_\omega(z_1-z_2)}, \tag{C4}$$

with $k_\omega = \frac{1}{c}\sqrt{\omega^2 - c^2\gamma_\lambda^2}$. The in-phase and out-of-phase components contribute *fieldlike* and *dampinglike* torques, respectively. In high quality waveguides, we can tune them by the positions of the two magnets.

Linearizing the coupled LLG equations and neglecting the small intrinsic Gilbert damping α_G yields (summation on $\eta = \{x, z\}$)

$$\begin{aligned}
&\omega M_{1,x} - (i\gamma\mu_0H_{\rm eff,1} + \omega\alpha^r_{1,z})M_{1,z} - J_{z\eta}M_{2,\eta} = 0,\\
&\omega M_{1,z} + (i\gamma\mu_0H_{\rm eff,1} + \omega\alpha^r_{1,x})M_{1,x} + J_{x\eta}M_{2,\eta} = 0,\\
&\omega M_{2,x} - (i\gamma\mu_0H_{\rm eff,2} + \omega\alpha^r_{2,z})M_{2,z} - P_{z\eta}M_{1,\eta} = 0,\\
&\omega M_{2,z} + (i\gamma\mu_0H_{\rm eff,2} + \omega\alpha^r_{2,x})M_{2,x} + P_{x\eta}M_{1,\eta} = 0,
\end{aligned} \tag{C5}$$

where

$$J_{\delta\eta} = \frac{\gamma\mu_0^2V_sM_s}{v(k_\omega)}\mathscr{H}_{k_\omega,\delta}(\boldsymbol{\rho}_1)\mathscr{H}^*_{k_\omega,\eta}(\boldsymbol{\rho}_2)e^{ik_\omega(z_1-z_2)},$$

$$P_{\delta\eta} = \frac{\gamma\mu_0^2V_sM_s}{v(k_\omega)}\mathscr{H}_{-k_\omega,\delta}(\boldsymbol{\rho}_2)\mathscr{H}^*_{-k_\omega,\eta}(\boldsymbol{\rho}_1)e^{ik_\omega(z_1-z_2)}. \tag{C6}$$

In the rotating wave approximation and weak coupling, we recover the equation for the eigenmodes, Eq. (76),

$$(iJ_{zx} - iJ_{xz} + J_{xx} + J_{zz})(iP_{zx} - iP_{xz} + P_{xx} + P_{zz})/4 + \left(\omega - \omega_1 + i\omega_1\alpha^r_1\right)\left(\omega - \omega_2 + i\omega_2\alpha^r_2\right) = 0, \tag{C7}$$

where $\omega_i = \gamma\mu_0H_{{\rm eff},i}$ and $\alpha^r_i = (\alpha^r_{i,x} + \alpha^r_{i,z})/2$. While equivalent, this method becomes tedious when considering many coupled magnetic spheres.

[1] B. Lenk, H. Ulrichs, F. Garbs, and M. Muenzenberg, Phys. Rep. **507**, 107 (2011).
[2] A. V. Chumak, V. I. Vasyuchka, A. A. Serga, and B. Hillebrands, Nat. Phys. **11**, 453 (2015).
[3] D. Grundler, Nat. Nanotech. **11**, 407 (2016).
[4] V. E. Demidov, S. Urazhdin, G. de Loubens, O. Klein, V. Cros, A. Anane, and S. O. Demokritov, Phys. Rep. **673**, 1 (2017).
[5] H. Chang, P. Li, W. Zhang, T. Liu, A. Hoffmann, L. Deng, and M. Wu, IEEE Magn. Lett. **5**, 6700104 (2014).
[6] Y. Tabuchi, S. Ishino, A. Noguchi, T. Ishikawa, R. Yamazaki, K. Usami, and Y. Nakamura, Science **349**, 405 (2015).
[7] Y. Tserkovnyak, A. Brataas, and G. E. W. Bauer, Phys. Rev. Lett. **88**, 117601 (2002).
[8] Y. Tserkovnyak, A. Brataas, G. E. W. Bauer, and B. I. Halperin, Rev. Mod. Phys. **77**, 1375 (2005).
[9] T. Yu, C. P. Liu, H. M. Yu, Ya. M. Blanter, and G. E. W. Bauer, Phys. Rev. B **99**, 134424 (2019).
[10] J. L. Chen, T. Yu, C. P. Liu, T. Liu, M. Madami, K. Shen, J. Y. Zhang, S. Tu, M. S. Alam, K. Xia, M. Z. Wu, G. Gubbiotti, Ya. M. Blanter, G. E. W. Bauer, and H. M. Yu, Phys. Rev. B **100**, 104427 (2019).
[11] T. Yu, Y. M. Blanter, and G. E. W. Bauer, Phys. Rev. Lett. **123**, 247202 (2019).
[12] Y. Kubo, F. R. Ong, P. Bertet, D. Vion, V. Jacques, D. Zheng, A. Dréau, J.-F. Roch, A. Auffeves, F. Jelezko, J. Wrachtrup, M. F. Barthe, P. Bergonzo, and D. Esteve, Phys. Rev. Lett. **105**, 140502 (2010).
[13] R. Amsüss, C. Koller, T. Nöbauer, S. Putz, S. Rotter, K. Sandner, S. Schneider, M. Schramböck, G. Steinhauser, H. Ritsch, J. Schmiedmayer, and J. Majer, Phys. Rev. Lett. **107**, 060502 (2011).
[14] D. I. Schuster, A. P. Sears, E. Ginossar, L. DiCarlo, L. Frunzio, J. J. L. Morton, H. Wu, G. A. D. Briggs, B. B. Buckley, D. D. Awschalom, and R. J. Schoelkopf, Phys. Rev. Lett. **105**, 140501 (2010).
[15] S. Probst, H. Rotzinger, S. Wünsch, P. Jung, M. Jerger, M. Siegel, A. V. Ustinov, and P. A. Bushev, Phys. Rev. Lett. **110**, 157001 (2013).
[16] Ö. O. Soykal and M. E. Flatté, Phy. Rev. Lett. **104**, 077202 (2010).
[17] H. Huebl, C. W. Zollitsch, J. Lotze, F. Hocke, M. Greifenstein, A. Marx, R. Gross, and S. T. B. Goennenwein, Phy. Rev. Lett. **111**, 127003 (2013).
[18] Y. Tabuchi, S. Ishino, T. Ishikawa, R. Yamazaki, K. Usami, and Y. Nakamura, Phy. Rev. Lett. **113**, 083603 (2014).
[19] X. Zhang, C.-L. Zou, L. Jiang, and H. X. Tang, Phy. Rev. Lett. **113**, 156401 (2014).
[20] X. Zhang, C.-L. Zou, N. Zhu, F. Marquardt, L. Jiang, and H. X. Tang, Nat. Comm. **6**, 8914 (2015).
[21] S. M. Rezende, E. Soares, and V. Jaccarino, in *Nineteenth Annual Conference on Magnetism and Magnetic Materials*, edited by H. C. Wolfe, C. D. Graham, and J. J. Rhyne, AIP Conf. Proc. No. 18 (AIP, New York, 1974), p. 1083.
[22] R. W. Sanders, D. Paquette, V. Jaccarino, and S. M. Rezende, Phys. Rev. B **10**, 132 (1974).
[23] B. M. Yao, T. Yu, Y. S. Gui, J. W. Rao, Y. T. Zhao, W. Lu, and C.-M. Hu, Commun. Phys. **2**, 161 (2019).
[24] N. Bloembergen and R. V. Pound, Phys. Rev. **95**, 8 (1954).

[25] M. A. W. Schoen, J. M. Shaw, H. T. Nembach, M. Weiler, and T. J. Silva, Phys. Rev. B **92**, 184417 (2015).
[26] J. D. Jackson, *Classical Electrodynamics* (Wiley, New York, 1998).
[27] P. Lodahl, S. Mahmoodian, S. Stobbe, A. Rauschenbeutel, P. Schneeweiss, J. Volz, H. Pichler, and P. Zoller, Nature (London) **541**, 473 (2017).
[28] Fam Le Kien, S. Dutta Gupta, K. P. Nayak, and K. Hakuta, Phys. Rev. A **72**, 063815 (2005).
[29] M. Scheucher, A. Hilico, E. Will, J. Volz, and A. Rauschenbeutel, Science **354**, 1577 (2016).
[30] B. Vermersch, P.-O. Guimond, H. Pichler, and P. Zoller, Phys. Rev. Lett. **118**, 133601 (2017).
[31] P. Schneeweiss, S. Zeiger, T. Hoinkes, A. Rauschenbeutel, and J. Volz, Opt. Lett. **42**, 85 (2017).
[32] C. A. Downing, J. C. López Carreño, F. P. Laussy, E. del Valle, and A. I. Fernández-Domínguez, Phys. Rev. Lett. **122**, 057401 (2019).
[33] A. G. Gurevich, Radiotekh. Elektron **8**, 780 (1963).
[34] A. G. Gurevich and G. A. Melkov, *Magnetization Oscillations and Waves* (CRC, New York, 1996).
[35] L. Martin, U.S. Patent No. US3426297A (1966).
[36] M. Harder, Y. Yang, B. M. Yao, C. H. Yu, J. W. Rao, Y. S. Gui, R. L. Stamps, and C.-M. Hu, Phys. Rev. Lett. **121**, 137203 (2018).
[37] B. M. Yao, T. Yu, X. Zhang, W. Lu, Y. S. Gui, C.-M. Hu, and Y. M. Blanter, Phys. Rev. B **100**, 214426 (2019).
[38] B. Zare Rameshti and G. E. W. Bauer, Phys. Rev. B **97**, 014419 (2018).
[39] A. Asenjo-García, M. Moreno-Cardoner, A. Albrecht, H. J. Kimble, and D. E. Chang, Phys. Rev. X **7**, 031024 (2017).
[40] Y.-X. Zhang and K. Mølmer, Phys. Rev. Lett. **122**, 203605 (2019).
[41] M. Moreno-Cardoner, D. Plankensteiner, L. Ostermann, D. E. Chang, and H. Ritsch, Phys. Rev. A **100**, 023806 (2019).
[42] P.-O. Guimond, A. Grankin, D. V. Vasilyev, B. Vermersch, and P. Zoller, Phys. Rev. Lett. **122**, 093601 (2019).
[43] G. Buonaiuto, R. Jones, B. Olmos, and I. Lesanovsky, New. J. Phys. **21**, 113021 (2019).
[44] J. Li, S. Y. Zhu, and G. S. Agarwal, Phys. Rev. Lett. **121**, 203601 (2018)
[45] S. Y. Yao and Z. Wang, Phys. Rev. Lett. **121**, 086803 (2018).
[46] T. Yu, Y.-X. Zhang, S. Sharma, X. Zhang, Y. M. Blanter, and G. E. W. Bauer, Phys. Rev. Lett. **124**, 107202 (2020).
[47] C. Kittel, Phys. Rev. **73**, 155 (1948).
[48] C. Kittel, *Quantum Theory of Solids* (Wiley, New York, 1963).
[49] L. D. Landau and E. M. Lifshitz, *Electrodynamics of Continuous Media*, 2nd ed. (Butterworth-Heinenann, Oxford, 1984).
[50] T. Holstein and H. Primakoff, Phys. Rev. **58**, 1098 (1940).
[51] A. Kamra and W. Belzig, Phys. Rev. Lett. **116**, 146601 (2016).
[52] T. Yu, S. Sharma, Ya. M. Blanter, and G. E. W. Bauer, Phys. Rev. B **99**, 174402 (2019).
[53] Y. Cao, P. Yan, H. Huebl, S. T. B. Goennenwein, and G. E. W. Bauer, Phys. Rev. B **91**, 094423 (2015).
[54] W. Yu, T. Yu, and G. E. W. Bauer (unpublished).
[55] C. W. Gardiner and M. J. Collett, Phys. Rev. A **31**, 3761 (1985).
[56] A. A. Clerk, M. H. Devoret, S. M. Girvin, F. Marquardt, and R. J. Schoelkopf, Rev. Mod. Phys. **82**, 1155 (2010).
[57] K. Mølmer, Y. Castin, and J. Dalibard, J. Opt. Soc. Am. B **10**, 524 (1993).
[58] C. W. Gardiner, Phys. Rev. Lett. **70**, 2269 (1993).
[59] Y. Xu, Y. Li, R. K. Lee, and A. Yariv, Phys. Rev. E **62**, 7389 (2000).
[60] S. Fan, P. R. Villeneuve, J. D. Joannopoulos, M. J. Khan, C. Manolatou, and H. A. Haus, Phys. Rev. B **59**, 15882 (1999).
[61] U. Fano, Phys. Rev. **124**, 1866 (1961).
[62] G. D. Mahan, *Many Particle Physics* (Plenum, New York, 1990).
[63] D. Gall, J. Appl. Phys. **119**, 085101 (2016).
[64] E. Šimánek and B. Heinrich, Phys. Rev. B **67**, 144418 (2003).
[65] A. A. Abrikosov, L. P. Gorkov, and I. E. Dzyaloshinski, *Methods of Quantum Field Theory in Statistical Physics* (Prentice Hall, Englewood Cliffs, NJ, 1963).
[66] A. L. Fetter and J. D. Walecka, *Quantum Theory of Many Particle Systems* (McGraw-Hill, New York, 1971).
[67] H. Haug and A. P. Jauho, *Quantum Kinetics in Transport and Optics of Semiconductors* (Springer, Berlin, 1996).
[68] N. Hatano and D. R. Nelson, Phys. Rev. Lett. **77**, 570 (1996).
[69] C. M. Bender, D. C. Brody, and H. F. Jones, Phys. Rev. Lett. **89**, 270401 (2002).
[70] C. M. Bender, D. C. Brody, H. F. Jones, and B. K. Meister, Phys. Rev. Lett. **98**, 040403 (2007).
[71] D. Zhang, X.-Q. Luo, Y.-P. Wang, T.-F. Li, and J. Q. You, Nat. Commun. **8**, 1368 (2017).
[72] R. El-Ganainy, K. G. Makris, M. Khajavikhan, Z. H. Musslimani, S. Rotter, and D. N. Christodoulides, Nat. Phys. **14**, 11 (2018).
[73] Z. Gong, Y. Ashida, K. Kawabata, K. Takasan, S. Higashikawa, and M. Ueda, Phys. Rev. X. **8**, 031079 (2018).
[74] X. S. Yang, Y. Cao, and Y. Zhai, arXiv:1904.02492.
[75] S. Y. Yao, F. Song, and Z. Wang, Phys. Rev. Lett. **121**, 136802 (2018).
[76] H. Jiang, L. J. Lang, C. Yang, S. L. Zhu, and S. Chen, Phys. Rev. B **100**, 054301 (2019).